Non-linear effects

Hannes BARTOSIK and Yannis PAPAPHILIPPOU
Accelerator and Beam Physics group
Beams Department
CERN

Joint University Accelerator School

Archamps, FRANCE

3 February 2017

Contents of the 2nd lecture

- Resonances and the path to chaos
  - Topology of 3rd and 4th order resonance
  - Path to chaos and resonance overlap
  - Dynamic aperture simulations
- Frequency map analysis
  - NAFF algorithm
  - Aspects of frequency maps
  - Frequency and diffusion maps for the LHC
  - Frequency map for lepton rings
  - Working point choice
  - Beam-beam effect
- Experiments
  - Experimental frequency maps
  - Beam loss frequency maps
  - Space-charge frequency scan

Contents of the 2nd lecture

- Resonances and the path to chaos
  - Topology of 3rd and 4th order resonance
  - Path to chaos and resonance overlap
  - Dynamic aperture simulations
- Frequency map analysis
  - NAFF algorithm
  - Aspects of frequency maps
  - Frequency and diffusion maps for the LHC
  - Frequency map for lepton rings
  - Working point choice
  - Beam-beam effect
- Experiments
  - Experimental frequency maps
  - Beam loss frequency maps
  - Space-charge frequency scan

Poincaré Section

- Record the **particle coordinates** at one location (BPM)
- **Unperturbed** motion lies on a **circle** in normalized coordinates (simple rotation)

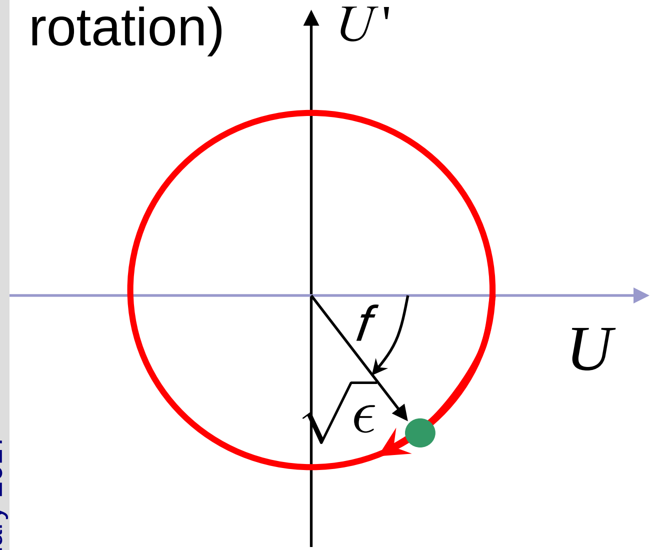

Poincaré Section:

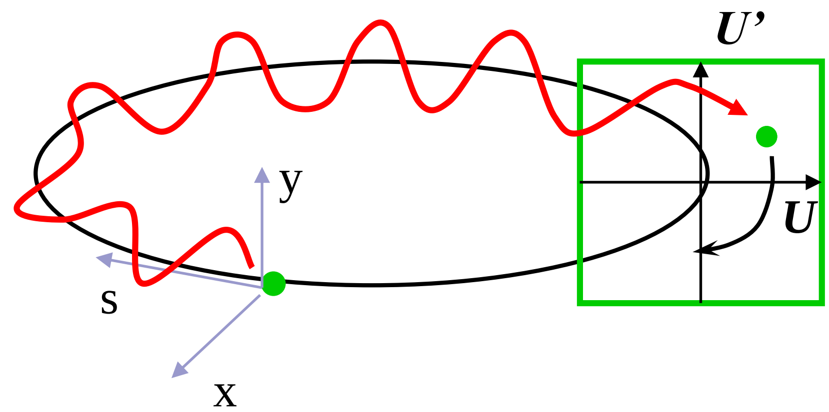

Poincaré Section

- Record the **particle coordinates** at one location (BPM)
- **Unperturbed** motion lies on a **circle** in normalized coordinates (simple rotation)

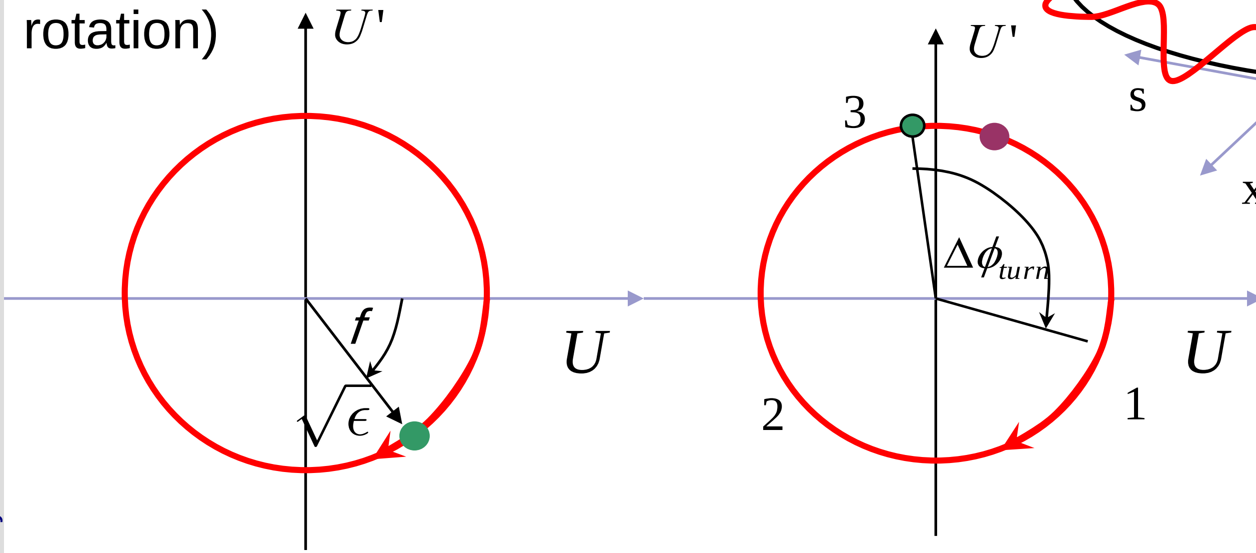

Poincaré Section:

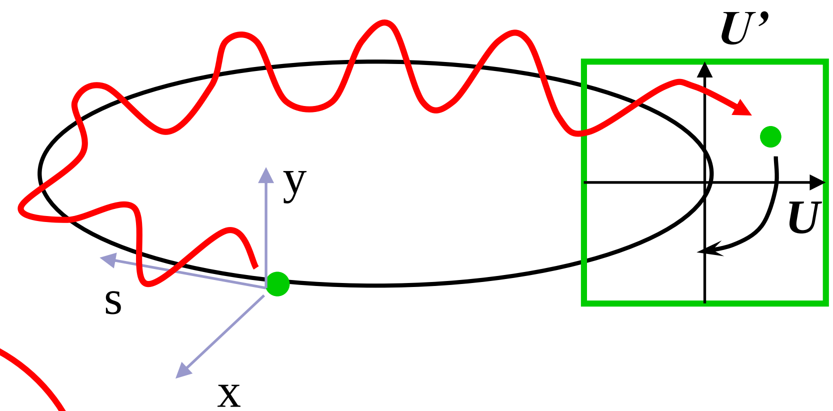

- **Resonance condition** corresponds to a periodic orbit or in **fixed points** in phase space

Poincaré Section

- Record the **particle coordinates** at one location (BPM)
- **Unperturbed** motion lies on a **circle** in normalized coordinates (simple rotation)

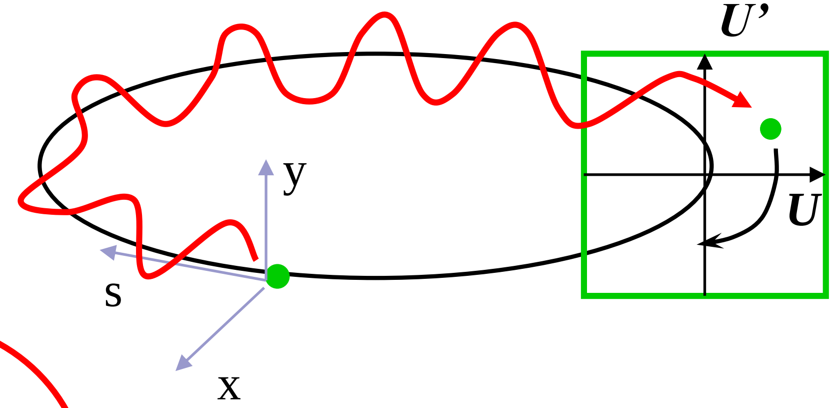

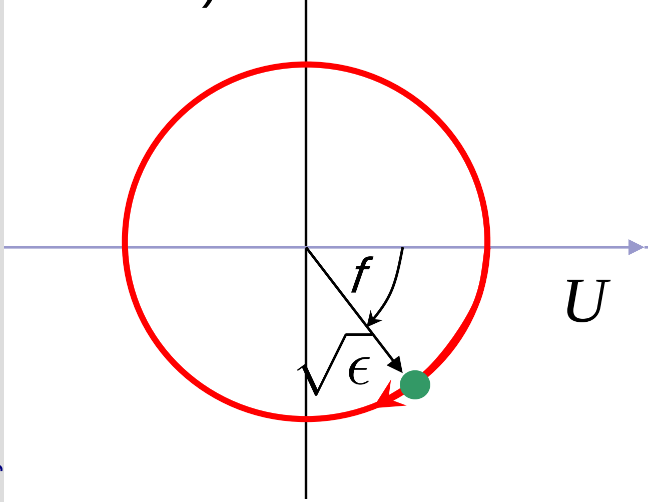

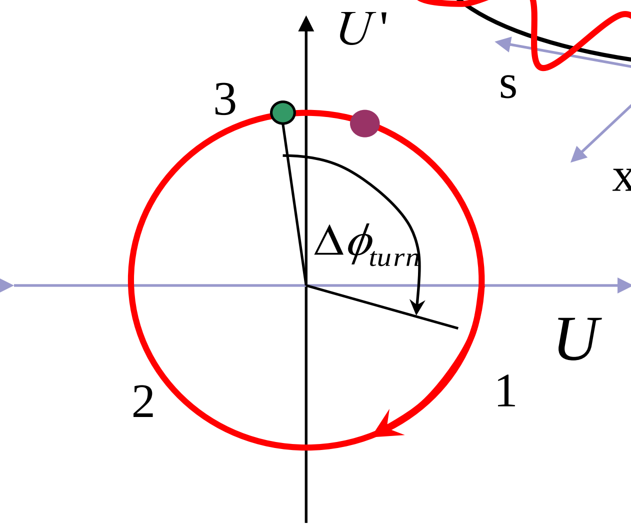

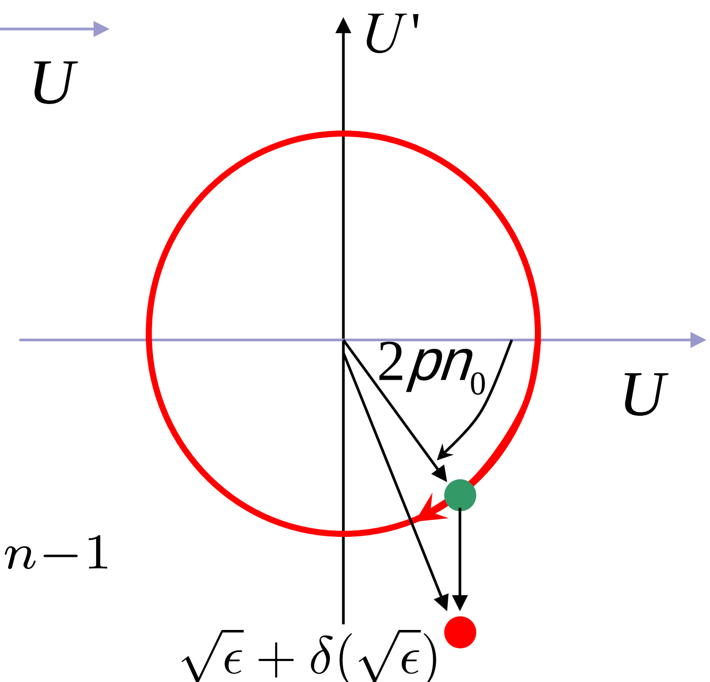

- **Resonance condition** corresponds to a periodic orbit or in **fixed points** in phase space
- For a **multi-pole perturbation** $\delta\mathcal{U}' = \overline{b_n}\mathcal{U}^{n-1}$
- The particle **does not lie on a circle**!

Phase space for sextupole perturbation

- Close to the periodic orbit, the motion is described by **circles** and the “invariant” is still almost an integral of motion
- Further away the **circles get distorted**, until the resonance condition is met
- It can be shown that **close to a resonance**, motion can be described by a **pendulum-like invariant**, and some analytical results can be derived

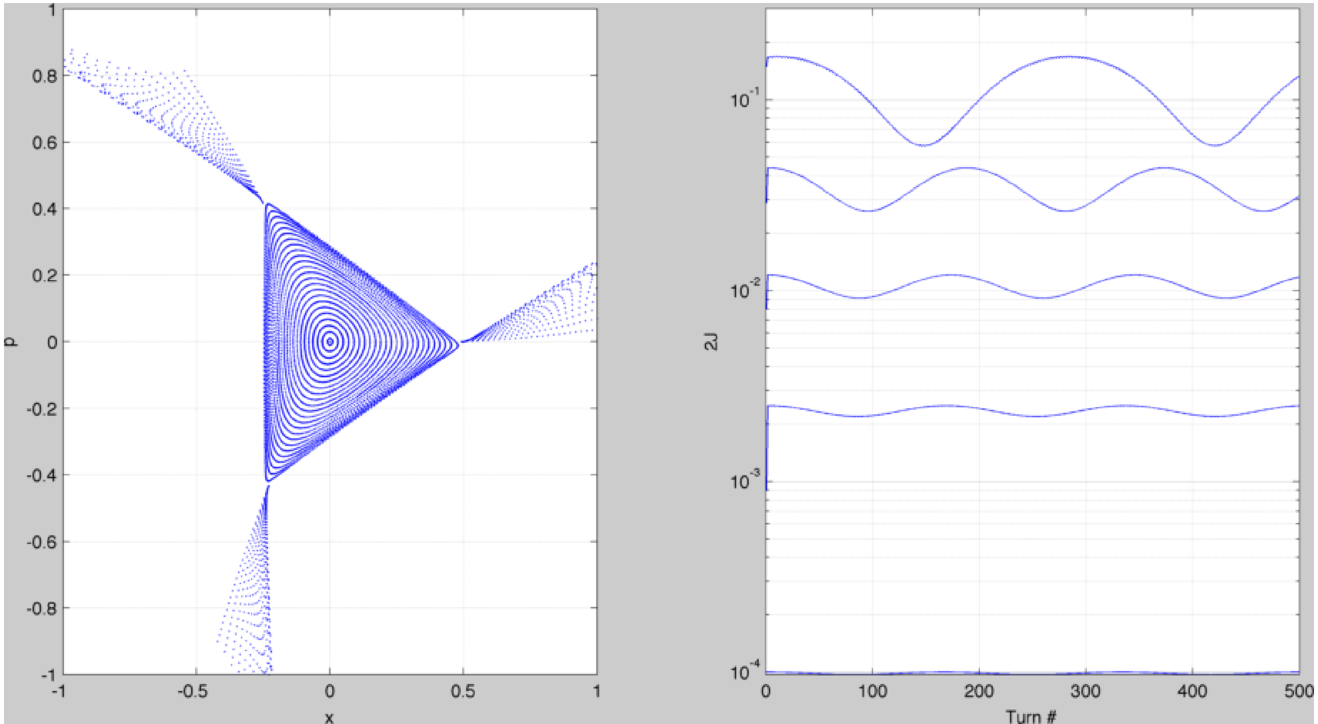

Fixed points for 3rd order resonance

- In the vicinity of a third order resonance, three fixed points can be found at

$$\psi_{20} = \frac{\pi}{3}, \quad \frac{3\pi}{3}, \quad \frac{5\pi}{3}, \quad J_{20} = \left(\frac{2\delta}{3A_{3p}}\right)^2$$

- For $\frac{\delta}{A_{3p}} > 0$ all three points are unstable
- Close to the elliptic one at $\psi_{20} = 0$ the motion in phase space is described by circles that they get more and more distorted to end up in the "**triangular**" **separatrix** uniting the unstable fixed points
- The tune separation from the resonance (**stop-band width**) is

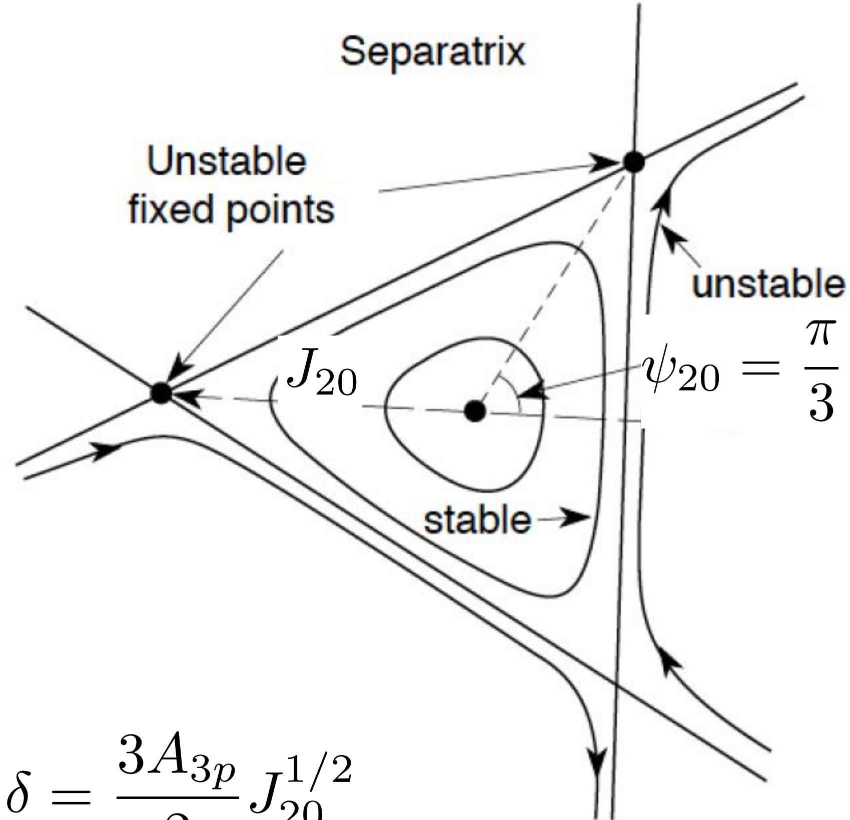

$$\delta = \frac{3A_{3p}}{2} J_{20}^{1/2}$$

Topology of an octupole resonance

- **Regular motion** near the center, with curves getting more deformed towards a **rectangular shape**
- The **separatrix** passes through 4 unstable fixed points, but motion seems well contained
- **Four stable fixed points** exist and they are surrounded by stable motion (**islands of stability**)
- Question: Can the **central fixed point** become **hyperbolic** (answer in the appendix)

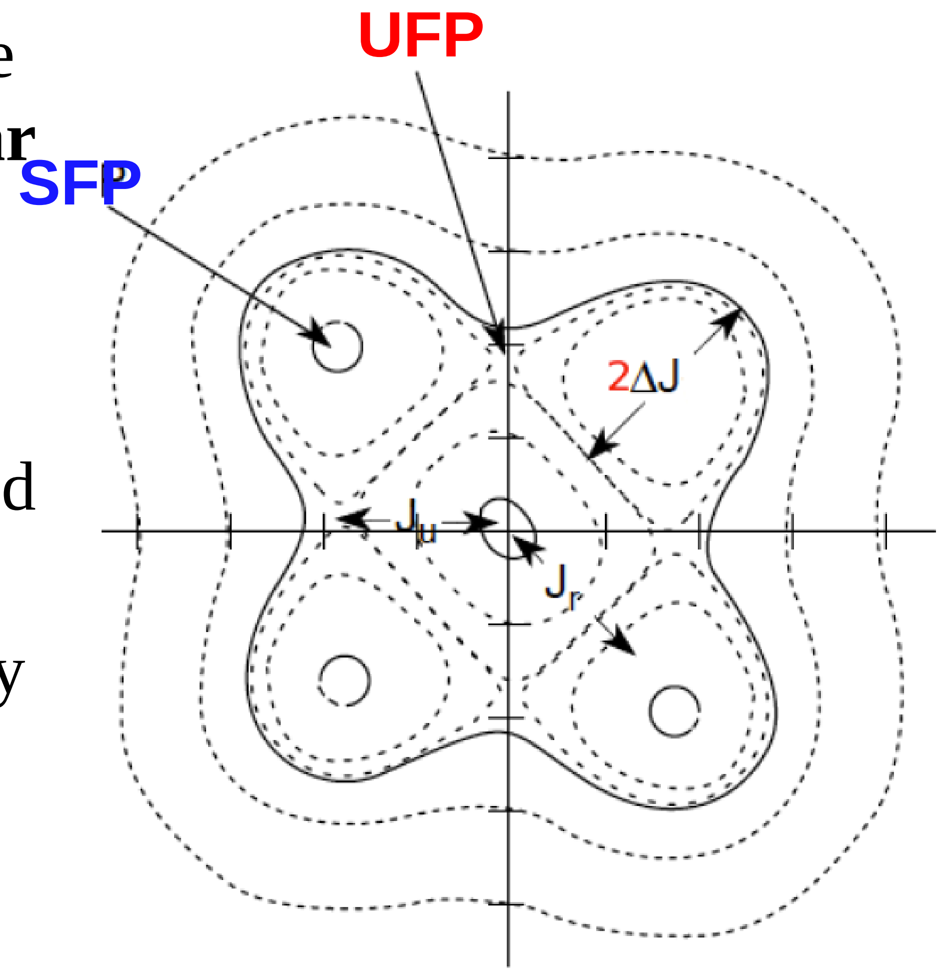

Path to chaos

- When **perturbation** becomes **higher**, motion around the **separatrix** becomes **chaotic** (producing **tongues** or **splitting** of the separatrix)
- **Unstable** fixed points are indeed the **source of chaos** when a perturbation is added

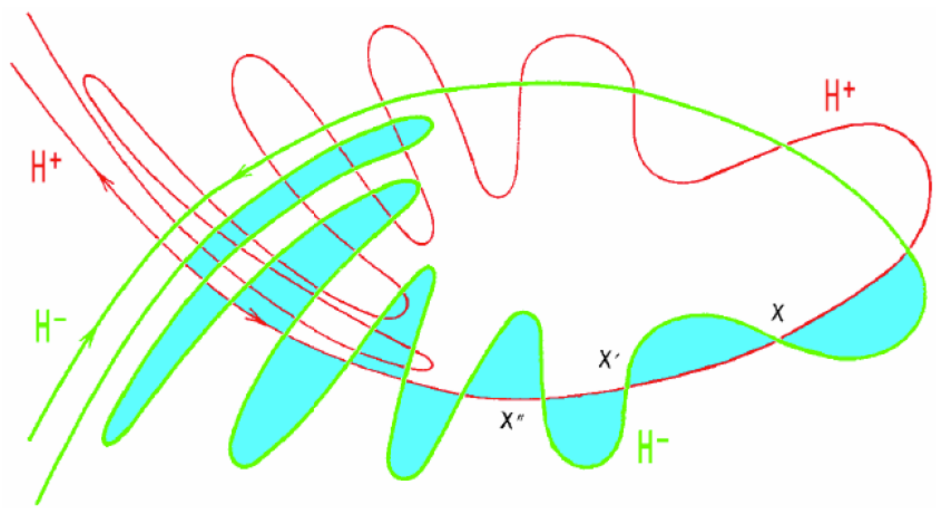

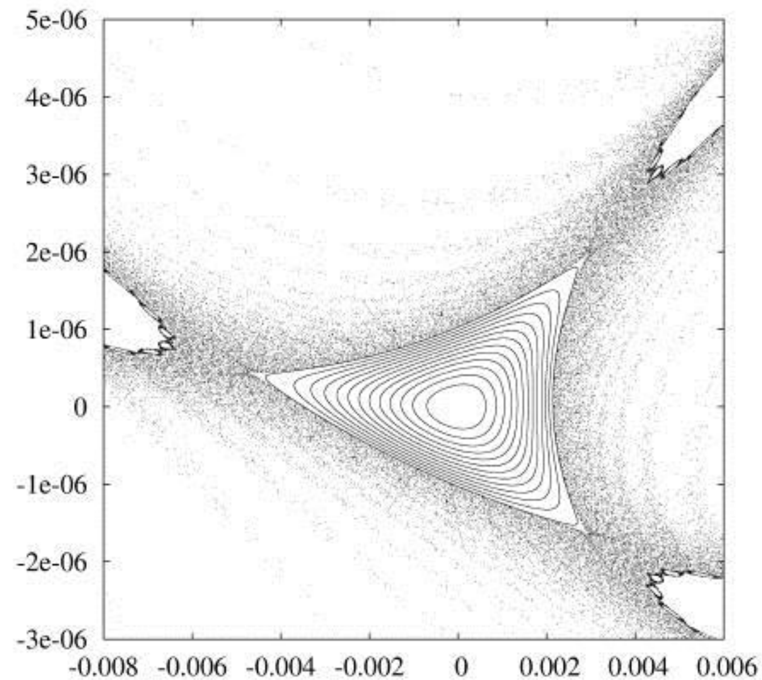

- **Poincare-Birkhoff** theorem states that under **perturbation** of a **resonance** only an **even number** of **fixed points** survives (**half stable** and the other **half unstable**)

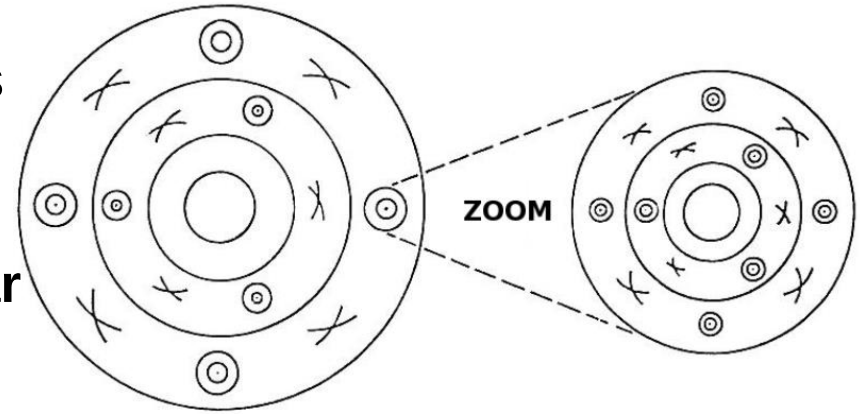

- **Themselves** get **destroyed** when perturbation gets **higher**, etc. (**self-similar** fixed points)
- Resonance **islands grow** and **resonances** can **overlap** allowing diffusion of pa

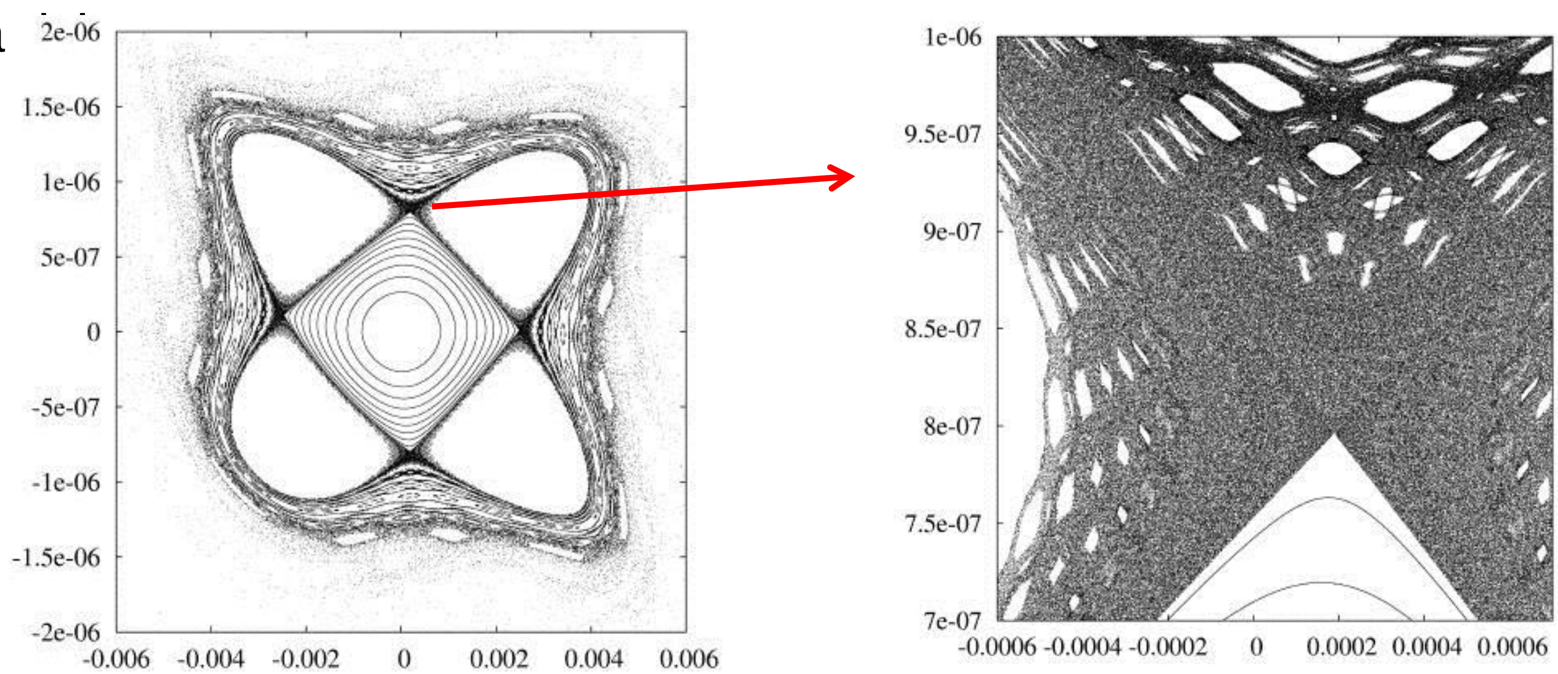

Resonance overlap criterion

- When perturbation grows, the resonance island width grows
- **Chirikov** (1960, 1979) proposed a **criterion** for the **overlap** of two **neighboring resonances** and the onset of orbit diffusion
- The **distance** between two resonances is $\delta \hat{J}_{1\ n,n'} = \dfrac{2\left(\frac{1}{n_1+n_2} - \frac{1}{n_1'+n_2'}\right)}{\left| \left. \frac{\partial^2 \bar{H}_0(\hat{\mathbf{J}})}{\partial \hat{J}_1^{\,2}} \right|_{\hat{J}_1=\hat{J}_{10}} \right|}$
- The **simple overlap criterion** is
  $$\Delta \hat{J}_{n\ max} + \Delta \hat{J}_{n'\ max} \geq \delta \hat{J}_{n,n'}$$
- Considering the **width** of **chaotic layer** and **secondary islands**, the "two thirds" rule apply $\Delta \hat{J}_{n\ max} + \Delta \hat{J}_{n'\ max} \geq \dfrac{2}{3} \delta \hat{J}_{n,n'}$
- The main limitation is the **geometrical nature** of the criterion (**difficulty** to be **extended** for **> 2 degrees of freedom**)

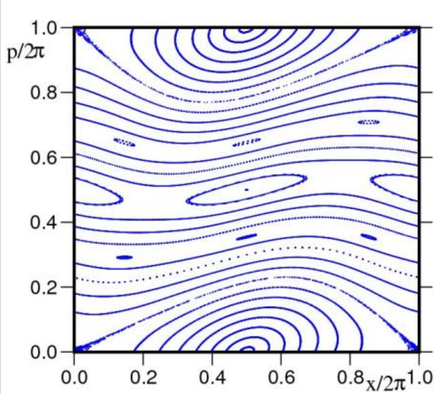

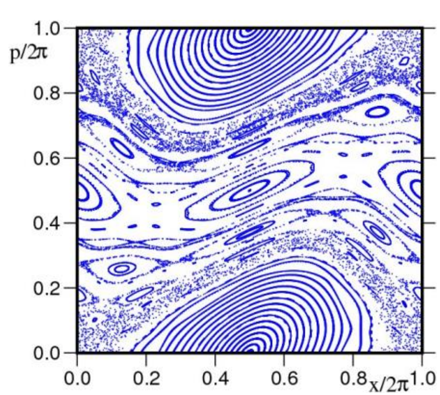

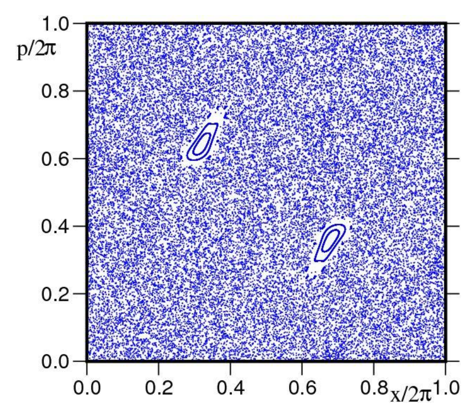

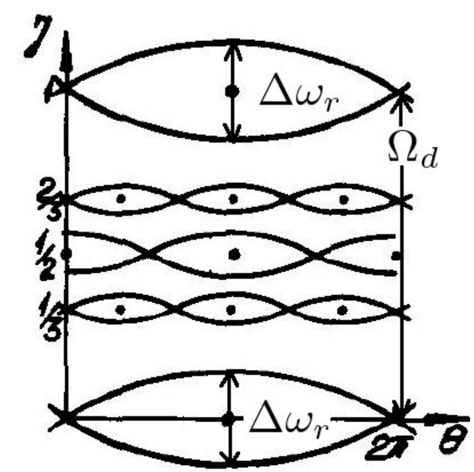

Dynamic Aperture

- The most direct way to evaluate the non-linear dynamics performance of a ring is the computation of **Dynamic Aperture**
- Particle motion due to multi-pole errors is generally non-bounded, so chaotic particles can **escape to infinity**
- This is not true for all non-linearities (e.g. the beam-beam force)
- Need a **symplectic** tracking code to follow particle trajectories (a lot of initial conditions) for a **number of turns** (depending on the given problem) until the particles start getting lost. This **boundary** defines the **Dynamic aperture**
- As multi-pole errors may not be completely known, one has to track through **several machine models** built by **random distribution** of these errors
- One could start with 4D (only transverse) tracking but certainly needs to simulate 5D (constant energy deviation) and finally 6D (synchrotron motion included)

Dynamic Aperture plots

- Dynamic aperture plots show the maximum initial values of stable trajectories in x-y coordinate space at a particular point in the lattice, for a range of energy errors.
  - The beam size can be shown on the same plot.
  - Generally, the goal is to allow some significant margin in the design - the measured dynamic aperture is often smaller than the predicted dynamic aperture.

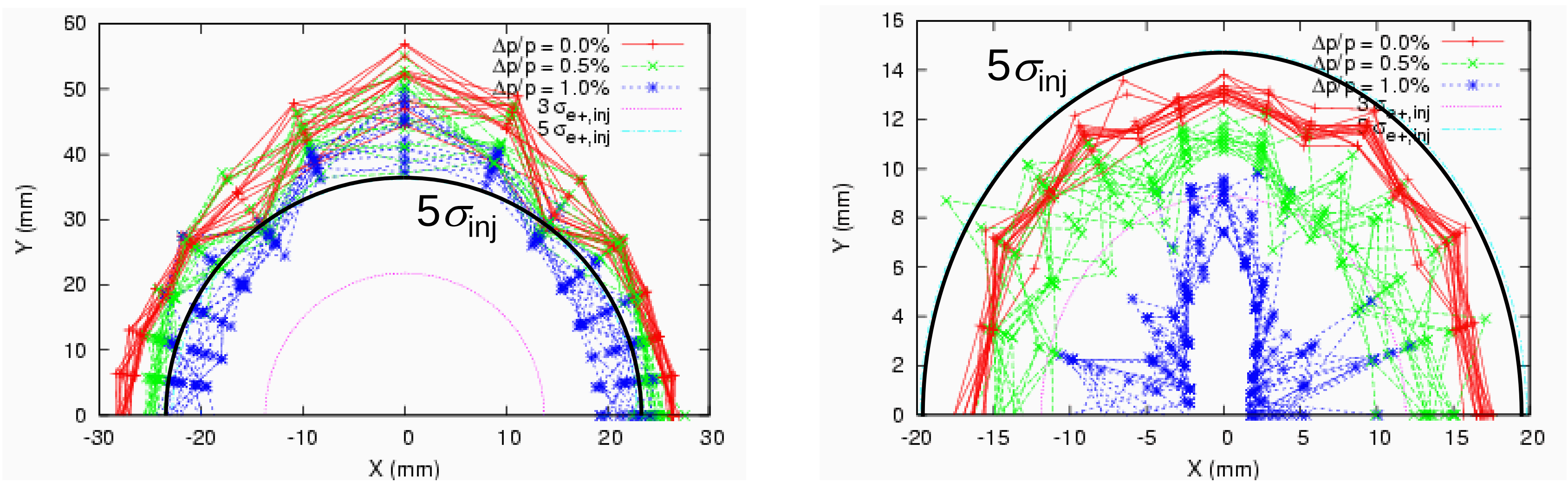

Dynamic aperture including damping

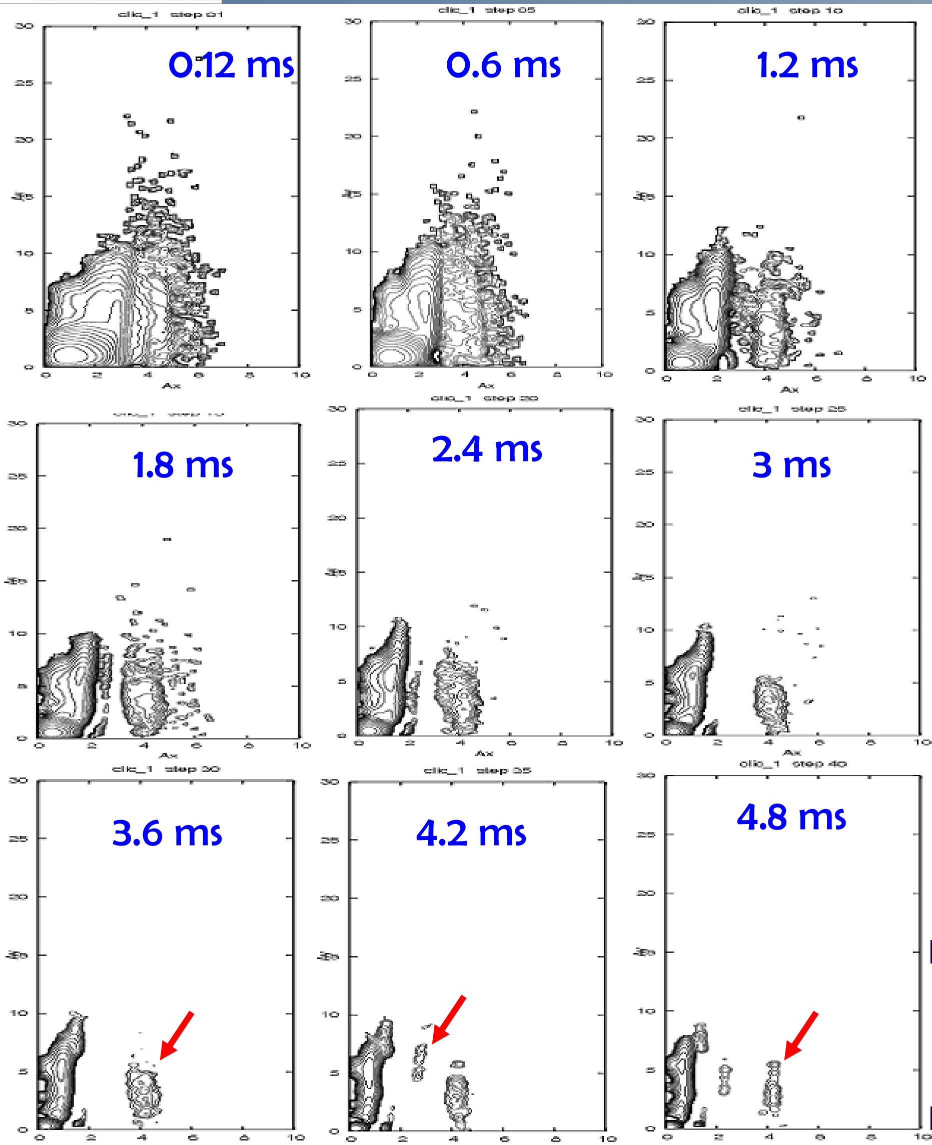

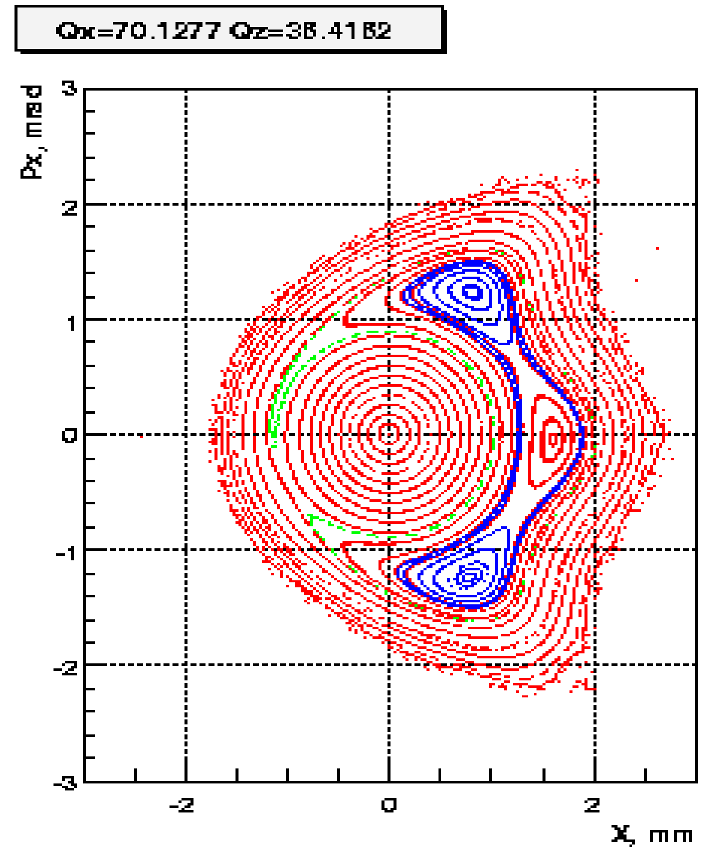

- Including radiation damping and excitation shows that 0.7% of the particles are lost during the damping
- Certain particles seem to damp away from the beam core, on resonance islands

DA scanning for the LHC

D.Pellegrini

- **Min. Dynamic Aperture (DA)** with **intensity** vs **crossing angle**, for **nominal optics** (**β*= 40 cm**) and **BCMS** beam (**2.5 μm** emittance), 15 units of chromaticity
- For **1.1×10^{11} p**
  - At **$\theta_c/2$ = 185 μrad** (~**12 σ** separation), DA around **6 σ** **(good lifetime observed)**
  - At **$\theta_c/2$ = 140 μrad** (~**9 σ** separation), DA below **5 σ** **(reduced lifetime observed)**
  - **Improvement** for low octupoles, low chromaticity and WP optimisation (observed in **operation**)

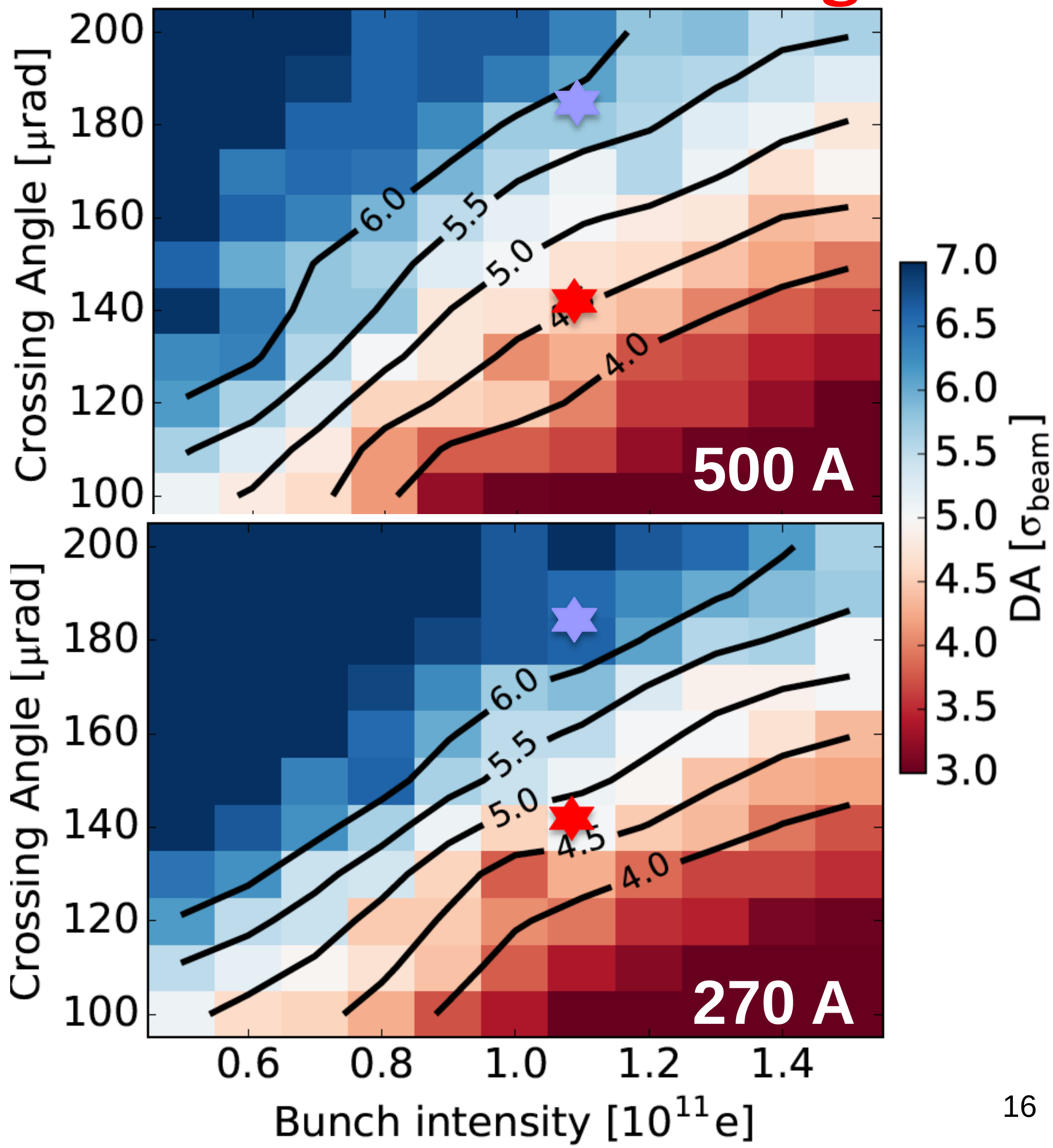

Genetic Algorithms for lattice optimisation

- MOGA –Multi Objective Genetic Algorithms are being recently used to optimise linear but also non-linear dynamics of electron low emittance storage rings
- Use knobs quadrupole strengths, chromaticity sextupoles and correctors with some constraints
- Target ultra-low horizontal emittance, increased lifetime and high dynamic aperture

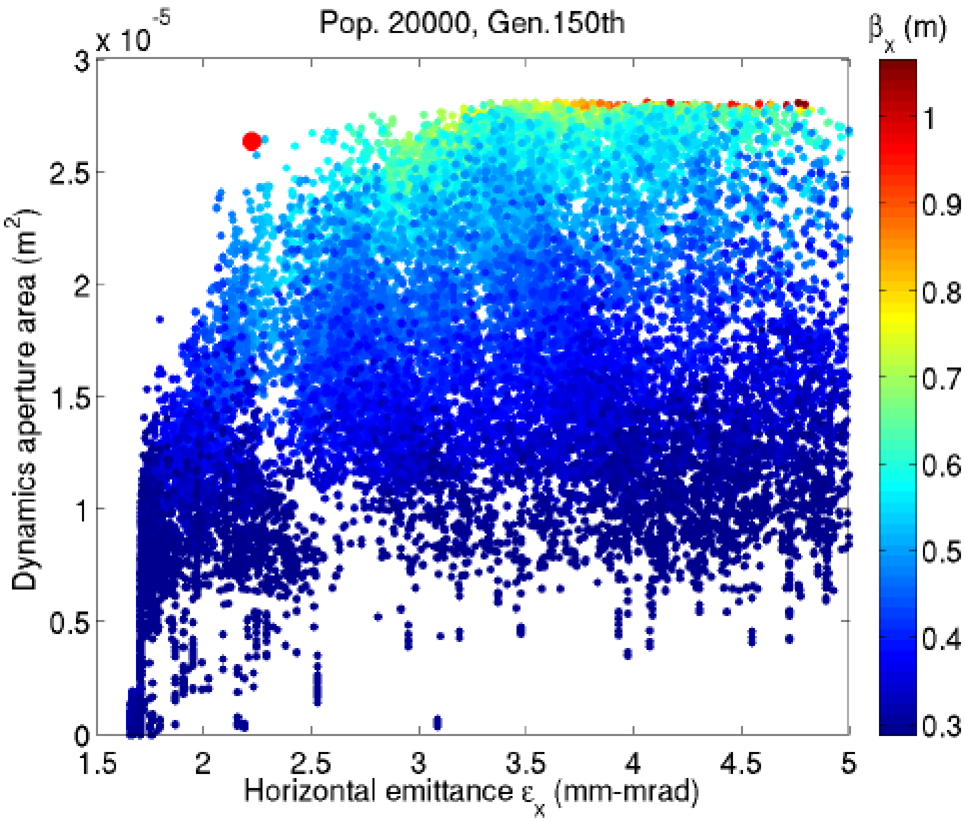

Measuring Dynamic Aperture

- During LHC design phase, DA target was 2x higher than collimator position, due to statistical fluctuation, finite mesh, linear imperfections, short tracking time, multi-pole time dependence, ripple and a 20% safety margin
- Better knowledge of the model led to good agreement between measurements and simulations for actual LHC
- Necessity to build an accurate magnetic model (from beam based measurements)

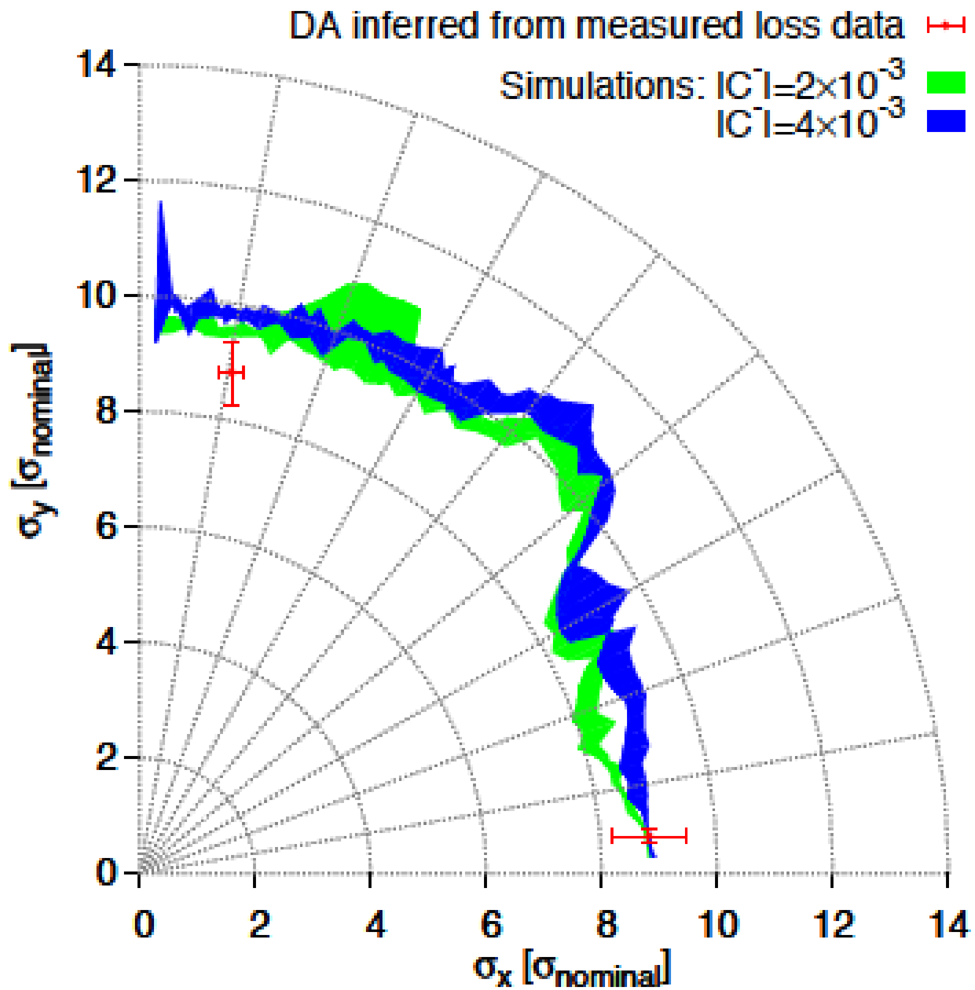

E.Mclean, PhD thesis, 2014

Contents of the 2nd lecture

- Resonances and the path to chaos
  - Topology of 3rd and 4th order resonance
  - Path to chaos and resonance overlap
  - Dynamic aperture simulations
- Frequency map analysis
  - NAFF algorithm
  - Aspects of frequency maps
  - Frequency and diffusion maps for the LHC
  - Frequency map for lepton rings
  - Working point choice
  - Beam-beam effect
- Experiments
  - Experimental frequency maps
  - Beam loss frequency maps
  - Space-charge frequency scan

Frequency map analysis

- Frequency Map Analysis (FMA) is a numerical method which springs from the studies of J. Laskar (Paris Observatory) putting in evidence the chaotic motion in the Solar Systems
- FMA was successively applied to several dynamical systems
  - Stability of Earth Obliquity and climate stabilization (Laskar, Robutel, 1993)
  - 4D maps (Laskar 1993)
  - Galactic Dynamics (Y.P and Laskar, 1996 and 1998)
  - Accelerator beam dynamics: lepton and hadron rings (Dumas, Laskar, 1993, Laskar, Robin, 1996, Y.P, 1999, Nadolski and Laskar 2001)

NAFF algorithm

- When a quasi-periodic function $f(t) = q(t) + ip(t)$ in the complex domain is given numerically, it is possible to recover a quasi-periodic approximation

$$f'(t) = \sum_{k=1}^{N} a'_k e^{i\omega'_k t}$$

  in a very precise way over a finite time span $[-T, T]$ several orders of magnitude more precisely than simple Fourier techniques
- This approximation is provided by the Numerical Analysis of Fundamental Frequencies – **NAFF** algorithm
- The frequencies ω'_k and complex amplitudes a'_k are computed through an iterative scheme.

Aspects of the frequency map

- In the vicinity of a resonance the system behaves like a pendulum
- Passing through the elliptic point for a fixed angle, a fixed frequency (or rotation number) is observed
- Passing through the hyperbolic point, a frequency jump is oberved

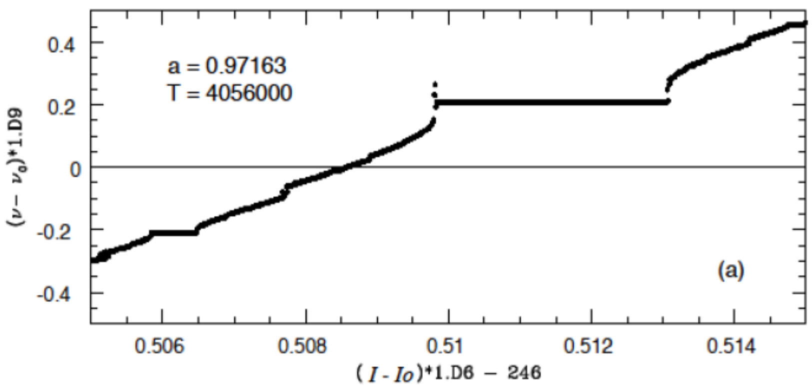

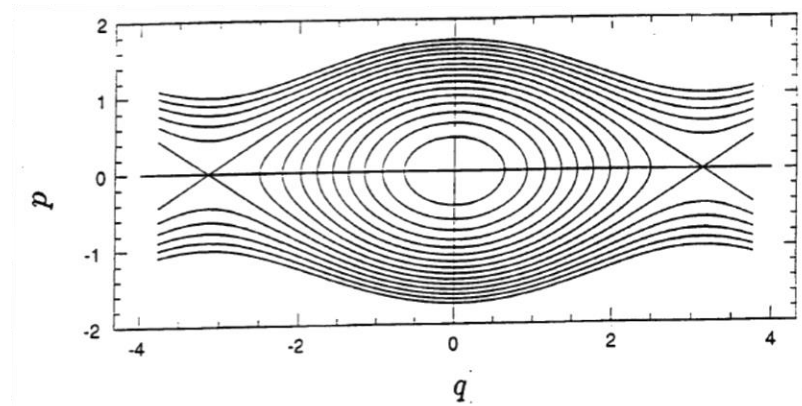

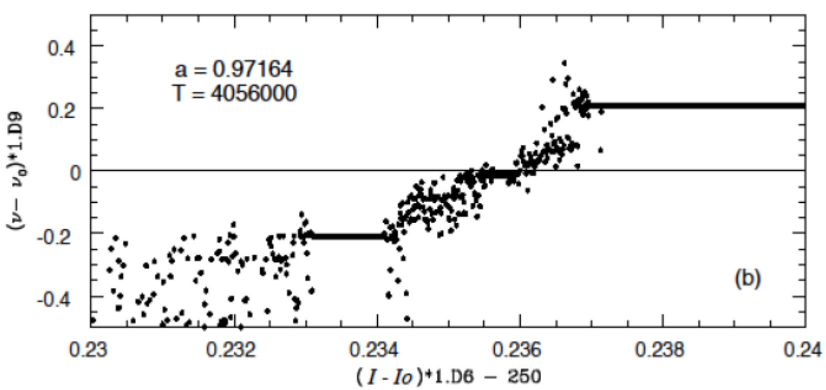

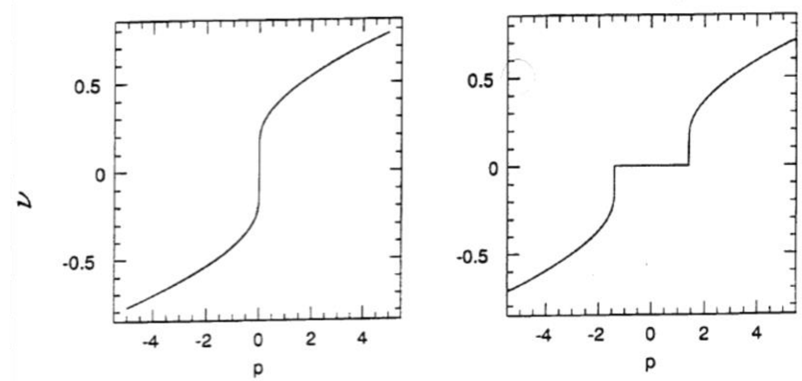

Building the frequency map

- Choose coordinates (x_i, y_i) with p_x and p_y=0
- Numerically integrate the phase trajectories through the lattice for sufficient number of turns
- Compute through NAFF Q_x and Q_y after sufficient number of turns
- Plot them in the tune diagram

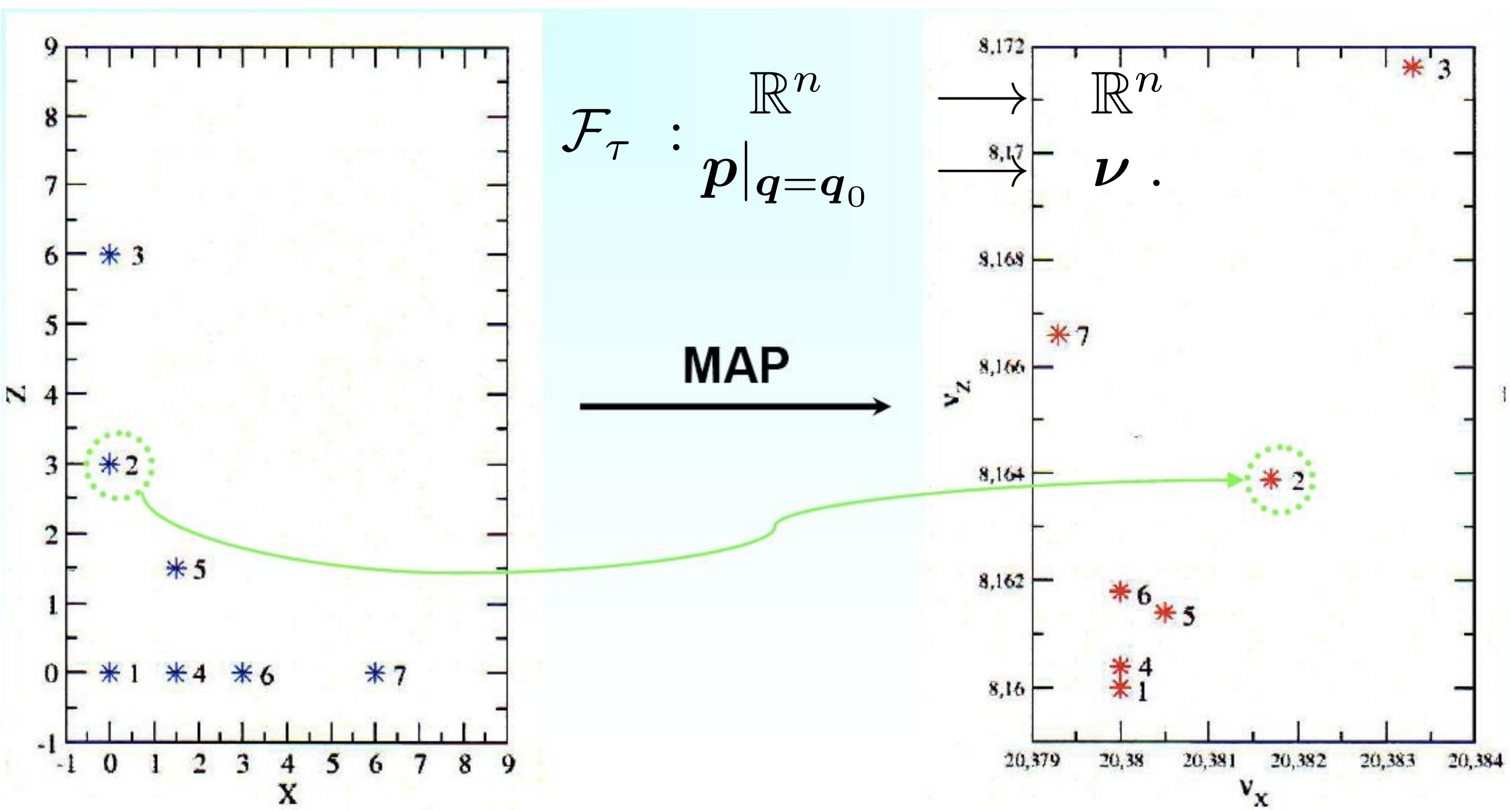

Frequency maps for the LHC

YP, PAC1999

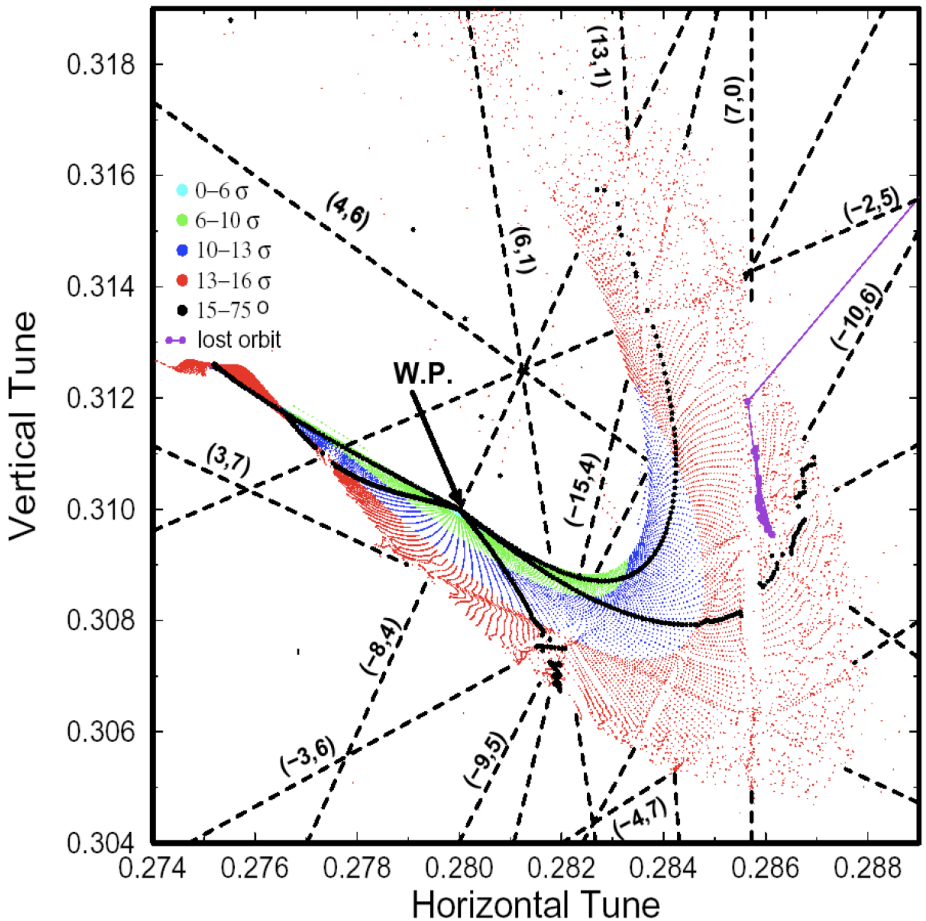

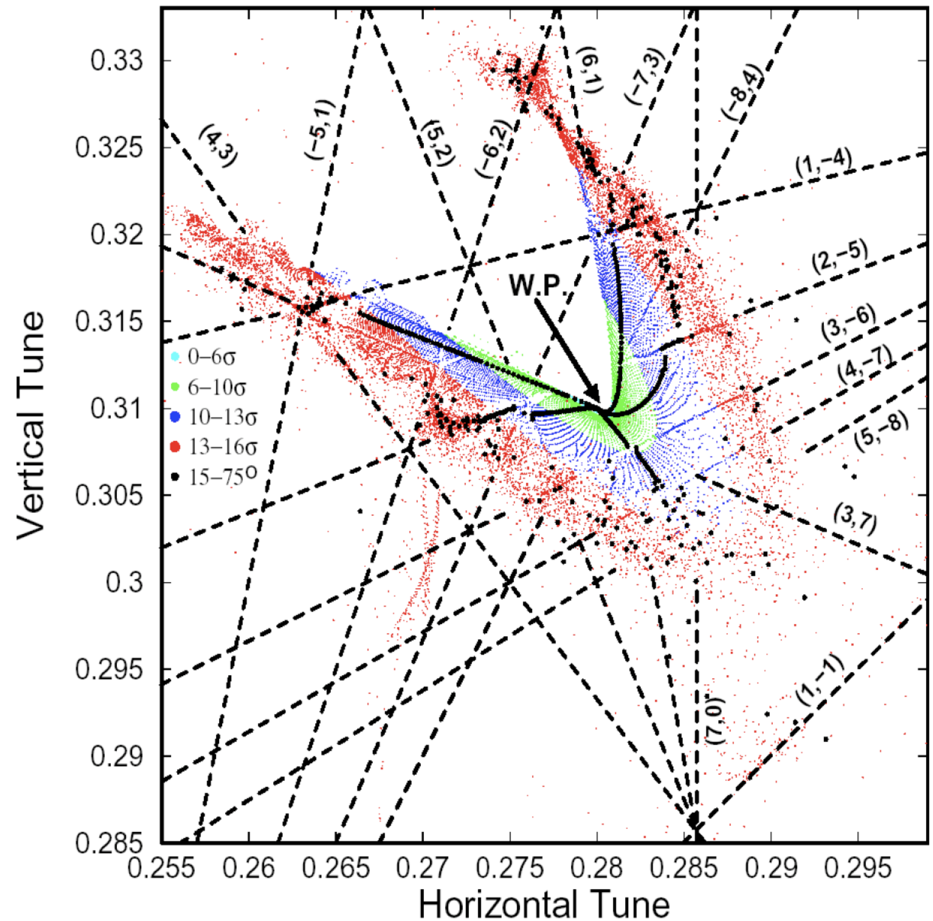

Frequency maps for the target error table (left) and an increased random skew octupole error in the super-conducting dipoles (right)

Diffusion Maps

J. Laskar, PhysicaD, 1993

- Calculate frequencies for two equal and successive time spans and compute frequency diffusion vector:

$$\boldsymbol{D}\big|_{t=\tau} = \boldsymbol{\nu}\big|_{t\in(0,\tau/2]} - \boldsymbol{\nu}\big|_{t\in(\tau/2,\tau]}$$

- Plot the initial condition space color-coded with the norm of the diffusion vector
- Compute a diffusion quality factor by averaging all diffusion coefficients normalized with the initial conditions radius

$$D_{QF} = \left\langle \frac{|\boldsymbol{D}|}{(I_{x0}^2 + I_{y0}^2)^{1/2}} \right\rangle_R$$

YP, PAC1999

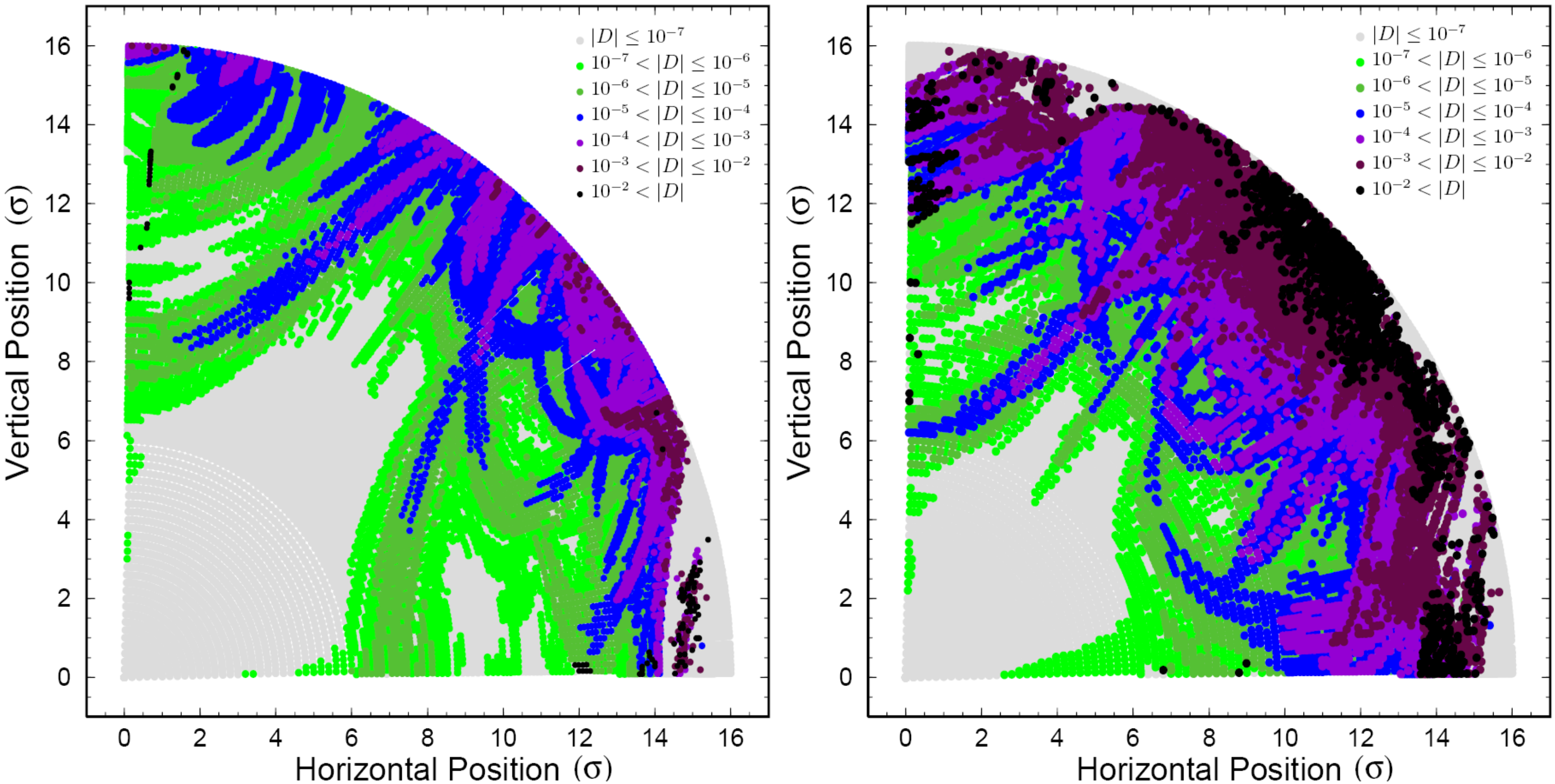

Diffusion maps for the target error table (left) and an increased random skew octupole error in the super-conducting dipoles (right)

Resonance free lattice for CLIC PDR

- Non linear optimization based on phase advance scan for minimization of resonance driving terms and tune-shift with amplitude

$$\left|\sum_{p=0}^{N_c-1} e^{ip(n_x\mu_{x,c}+n_y\mu_{y,c})}\right| = \sqrt{\frac{1-\cos\left[N_c(n_x\mu_{x,c}+n_y\mu_{y,c})\right]}{1-\cos(n_x\mu_{x,c}+n_y\mu_{y,c})}} = 0$$

$$\Downarrow$$

$$N_c(n_x\mu_{x,c}+n_y\mu_{y,c}) = 2k\pi$$

$$n_x\mu_{x,c}+n_y\mu_{y,c} \neq 2k'\pi$$

F.Antoniou, PhD thesis, 2103

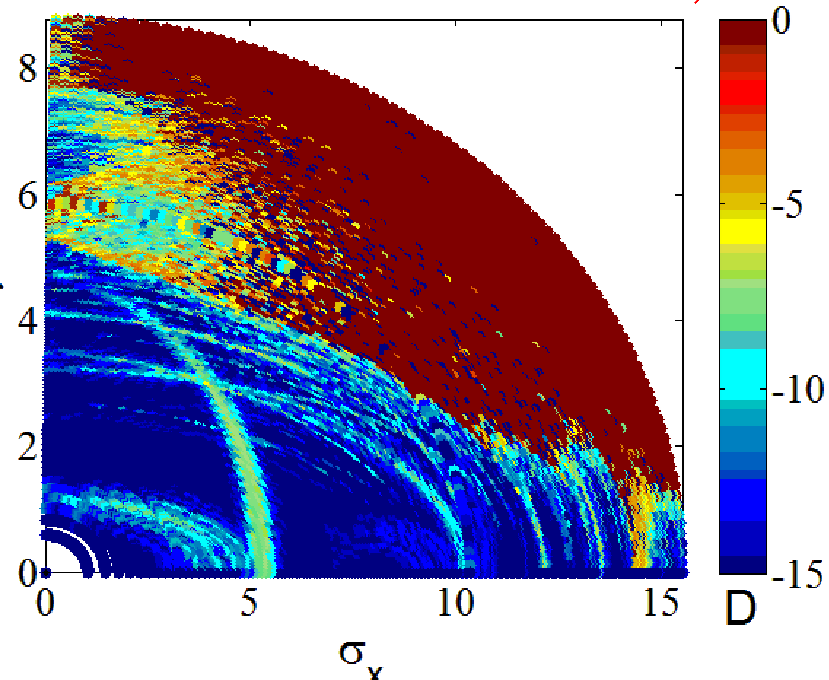

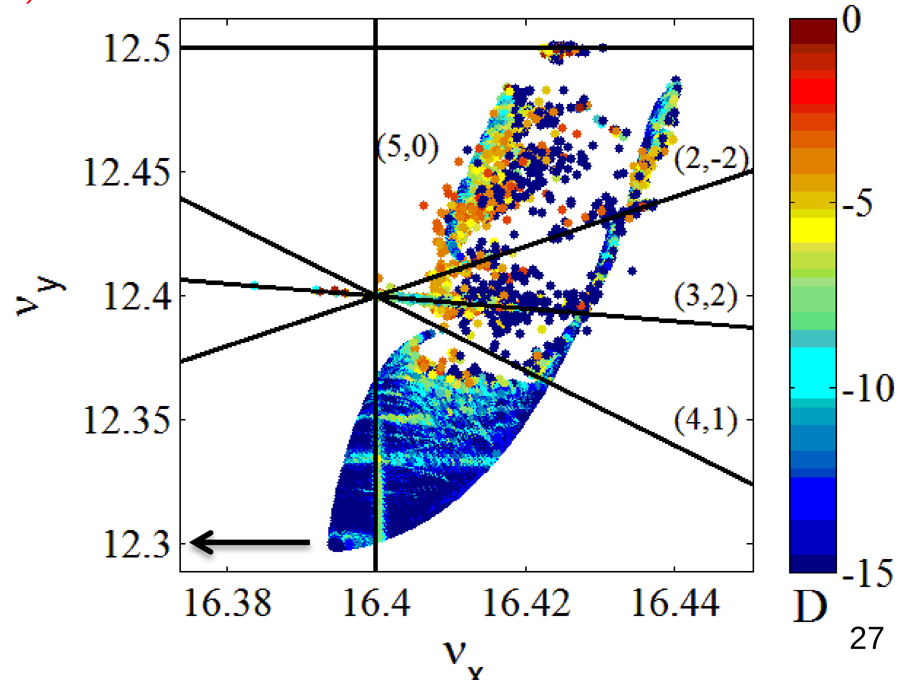

Frequency Map for the ESRF

- All dynamics represented in these two plots
- Regular motion represented by blue colors (close to zero amplitude particles or working point)

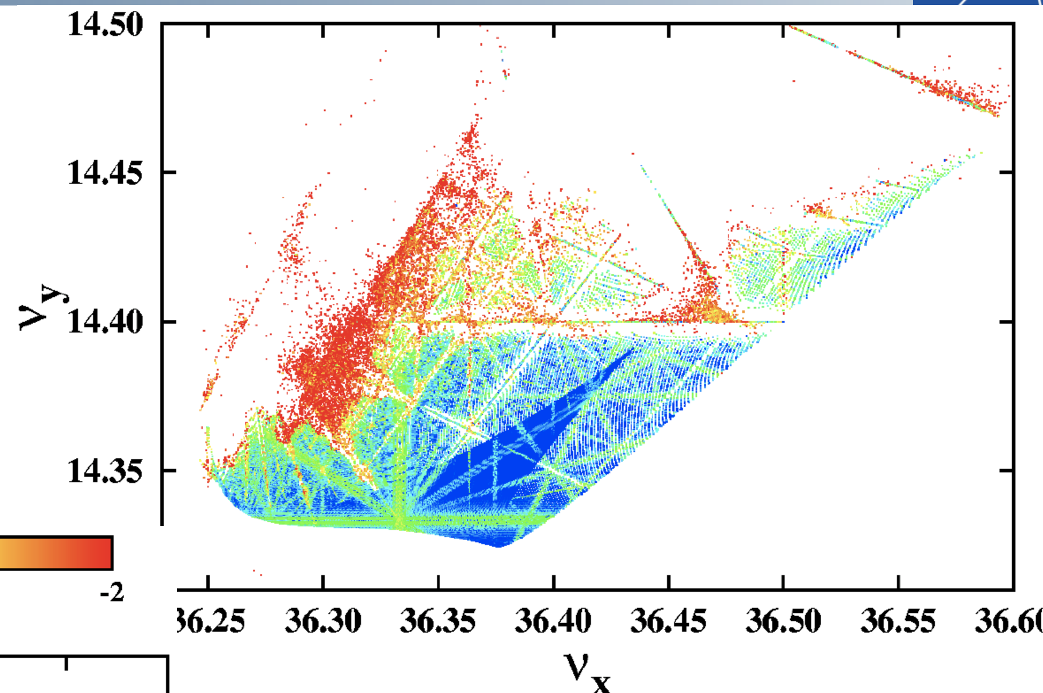

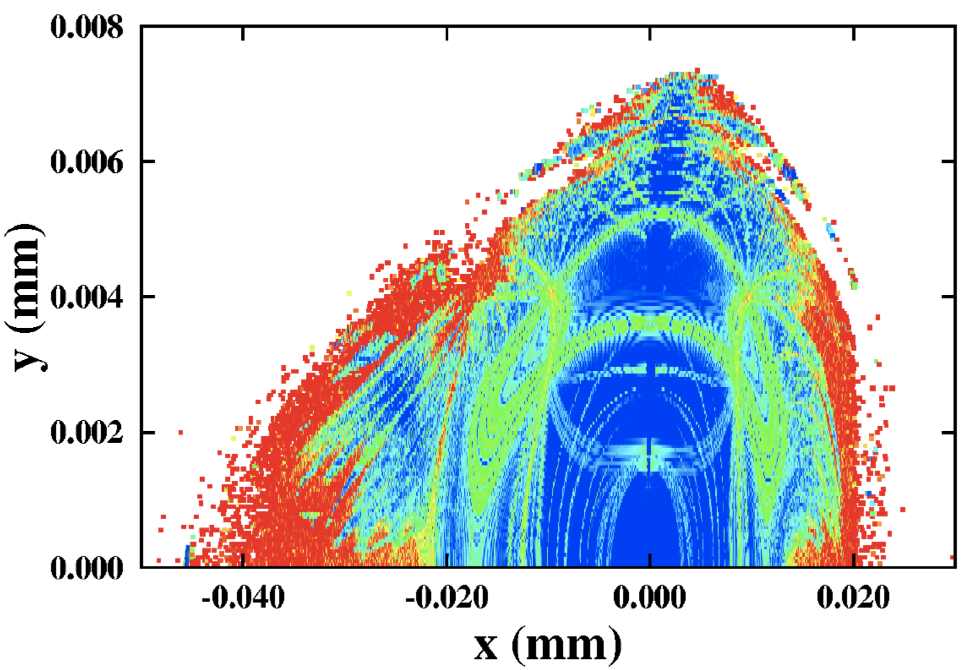

- Resonances appear as distorted lines in frequency space (or curves in initial condition space
- Chaotic motion is represented by red scattered particles and defines dynamic aperture of the machine

Example for the SNS ring: Working point (6.4,6.3)

- Integrate a large number of particles
- Calculate the tune with refined Fourier analysis
- Plot points to tune space

$$
\mathcal{F}_\tau : \begin{array}{ccc} \mathbb{R}^2 & \longrightarrow & \mathbb{R}^2 \\ (I_x, I_y)|_{p_x,p_y=0}, & \longrightarrow & (\nu_x, \nu_y) \end{array}
$$

SNS Working Point (Q_x,Q_y)=(6.4,6.3)

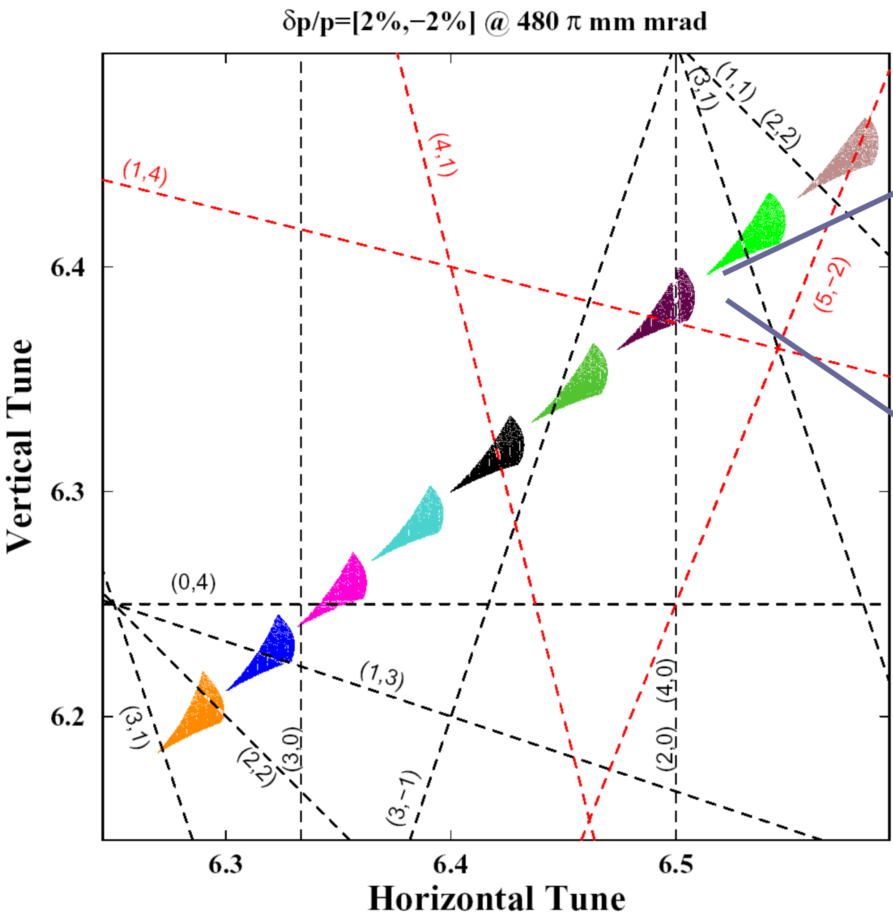

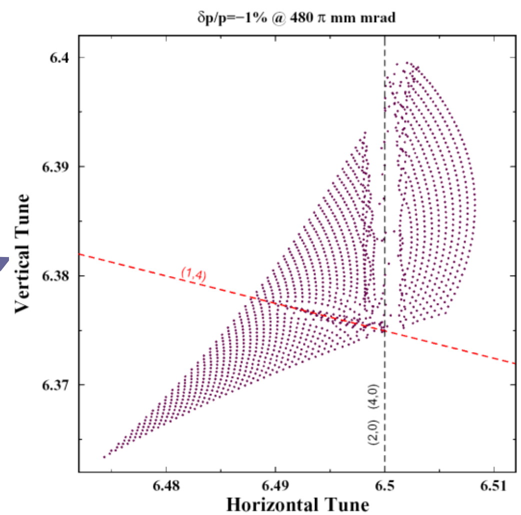

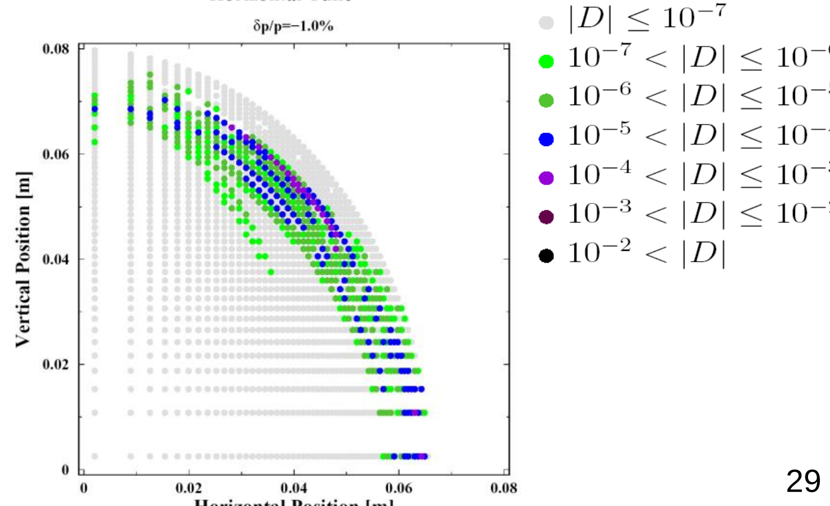

SNS Working point (6.23,5.24)

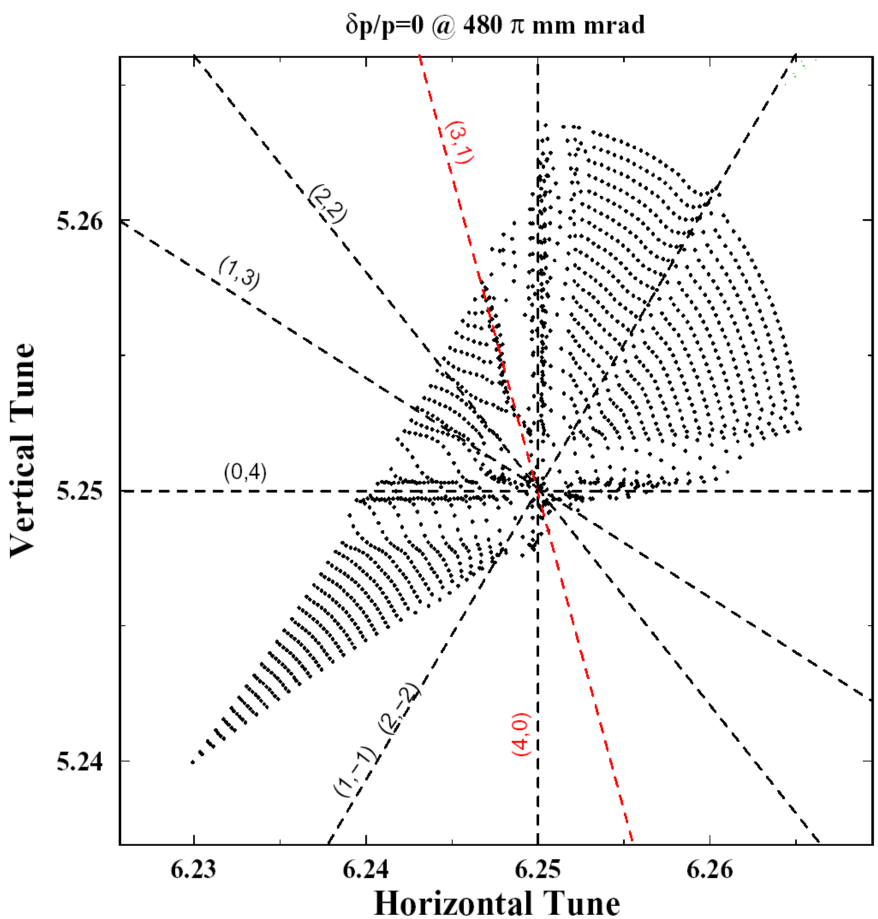

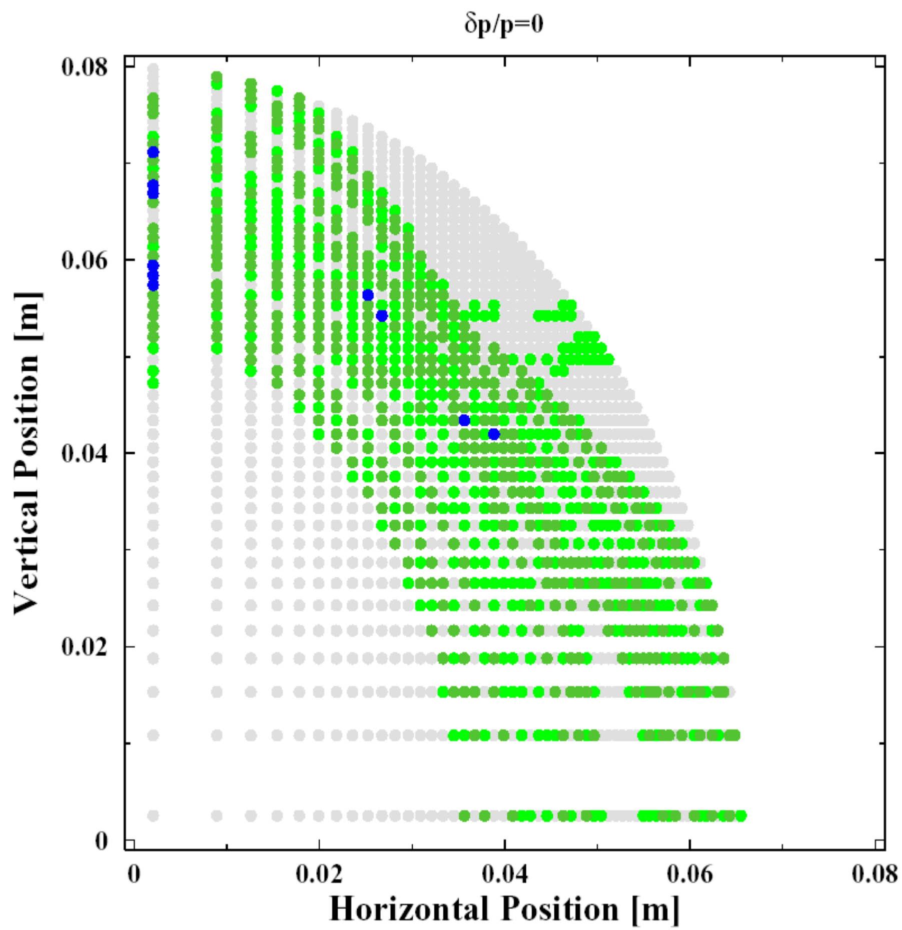

Working Point Comparison

Tune Diffusion quality factor

$$D_{QF} = \left\langle \frac{|\boldsymbol{D}|}{(I_{x0}^2 + I_{y0}^2)^{1/2}} \right\rangle_R$$

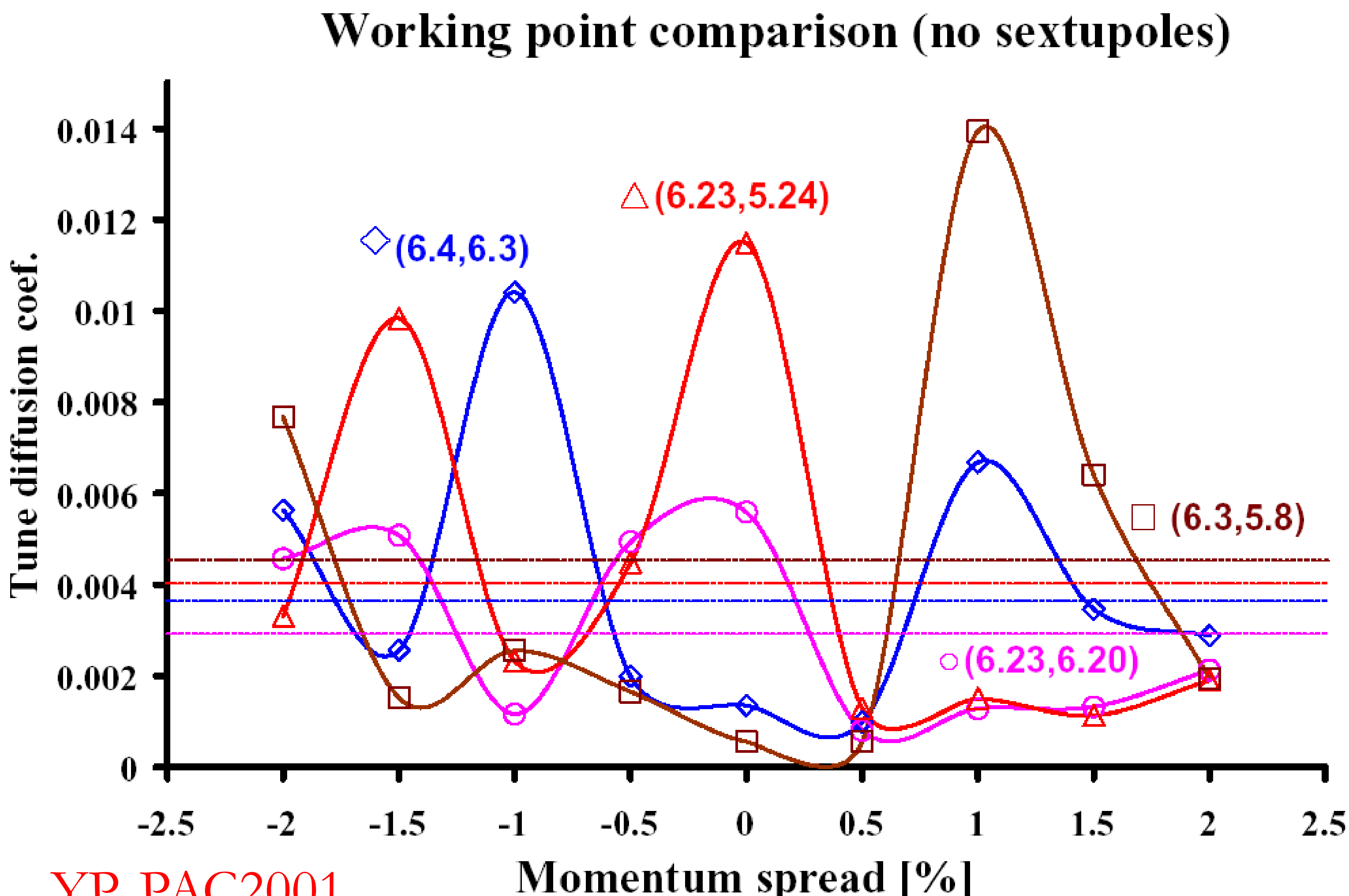

YP, PAC2001

Working point choice for SUPERB

- Figure of merit for choosing best working point is sum of diffusion rates with a constant added for every lost particle
- Each point is produced after tracking 100 particles
- Nominal working point had to be moved towards "blue" area

$$e^D = \sqrt{\frac{(\nu_{x,1} - \nu_{x,2})^2 + (\nu_{y,1} - \nu_{y,2})^2}{N/2}}$$

S. Liuzzo et al., IPAC 2012

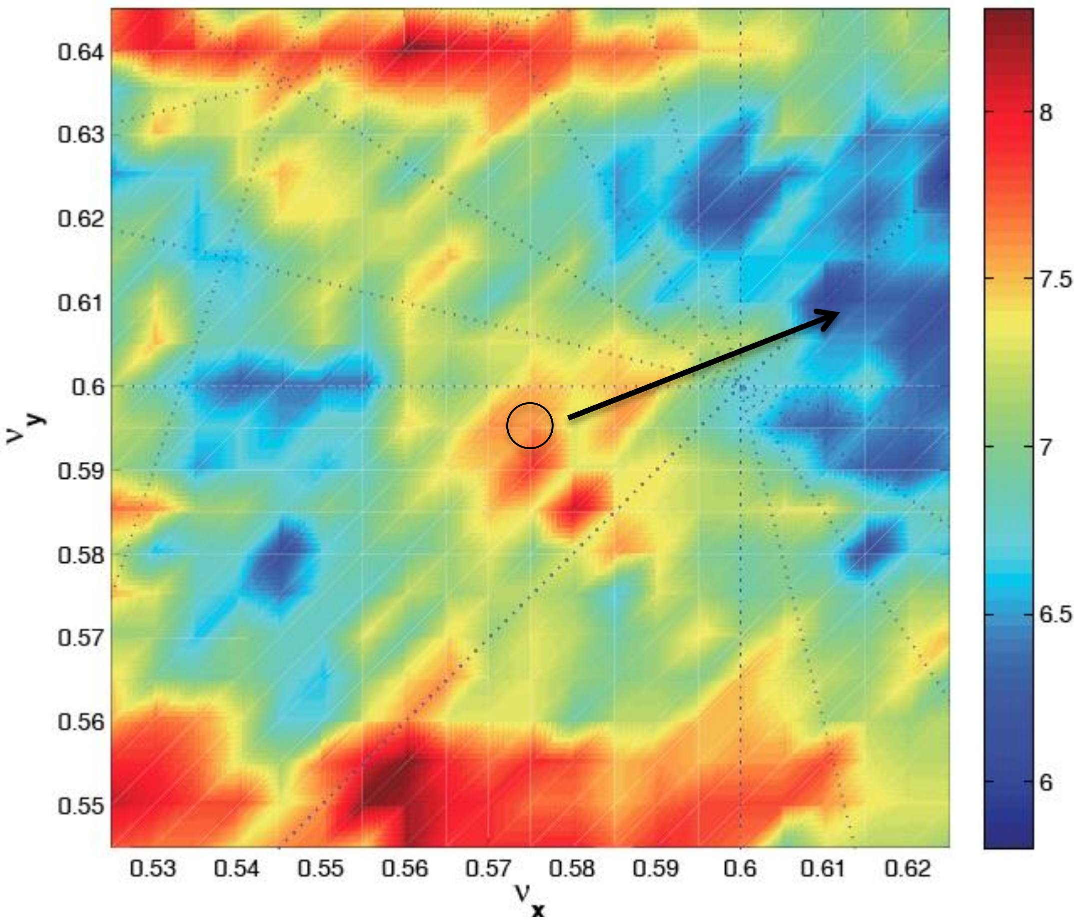

$$WPS = 0.1 N_{lost} + \sum e^D$$

Beam-Beam interaction

Variable	Symbol	Value
Beam energy	E	7 TeV
Particle species	$\cdots$	protons
Full crossing angle	θ_c	300 μrad
rms beam divergence	σ'_x	31.7 μrad
rms beam size	σ_x	15.9 μm
Normalized transv. rms emittance	$\gamma\varepsilon$	3.75 μm
IP beta function	β^*	0.5 m
Bunch charge	N_b	$(1\times10^{11}-2\times10^{12})$
Betatron tune	Q_0	0.31

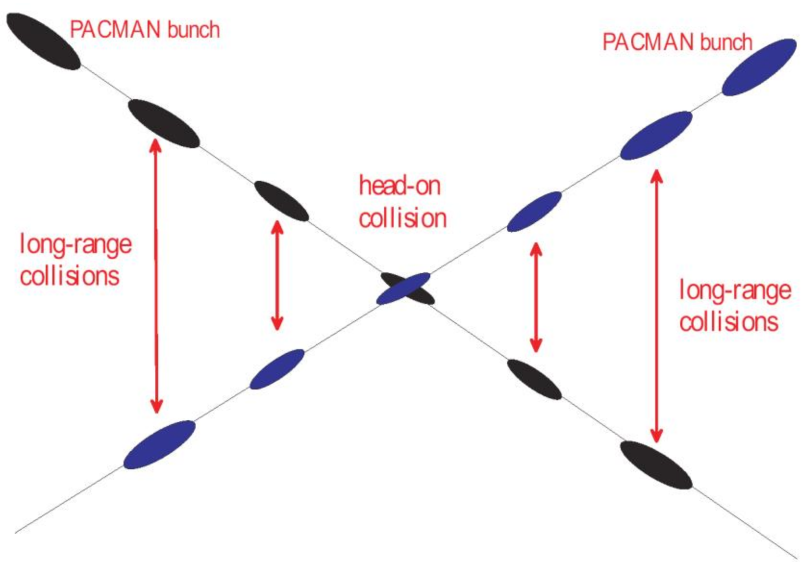

- Long range beam-beam interaction represented by a 4D kick-map

$$\Delta x = -\, n_{par} \frac{2r_p N_b}{\gamma} \left[\frac{x'+\theta_c}{\theta_t^2} \left(1 - e^{-\frac{\theta_t^2}{2\theta_{x,y}^2}}\right) - \frac{1}{\theta_c}\left(1 - e^{-\frac{\theta_c^2}{2\theta_{x,y}^2}}\right) \right]$$

$$\Delta y = -\, n_{par} \frac{2r_p N_b}{\gamma} \frac{y'}{\theta_t^2} \left(1 - e^{-\frac{\theta_t^2}{2\theta_{x,y}^2}}\right)$$

with $\quad \theta_t \equiv \left((x'+\theta_c)^2 + {y'}^2\right)^{1/2}$

Head-on vs Long range interaction

YP and F. Zimmermann, PRSTAB 1999, 2002

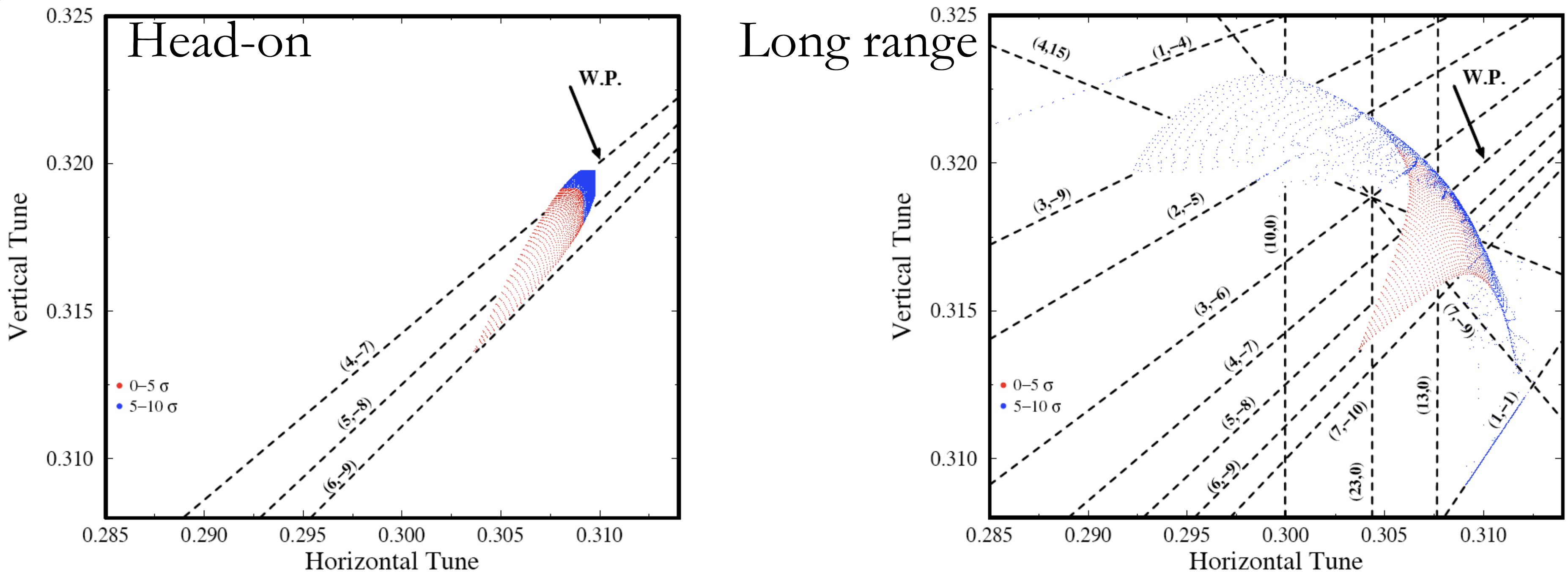

- Proved dominant effect of long range beam-beam effect
- Dynamic Aperture (around 6σ) located at the folding of the map (indefinite torsion)
- Dynamics dominated by the 1/r part of the force, reproduced by electrical wire, which was proposed for correcting the effect
- Experimental verification in SPS and installation to the LHC IPs

Wire compensation

- Current baring wire can **improve DA by 1-2 σ**
- Tests in the LHC during 2017-2018

Without correction | With correction

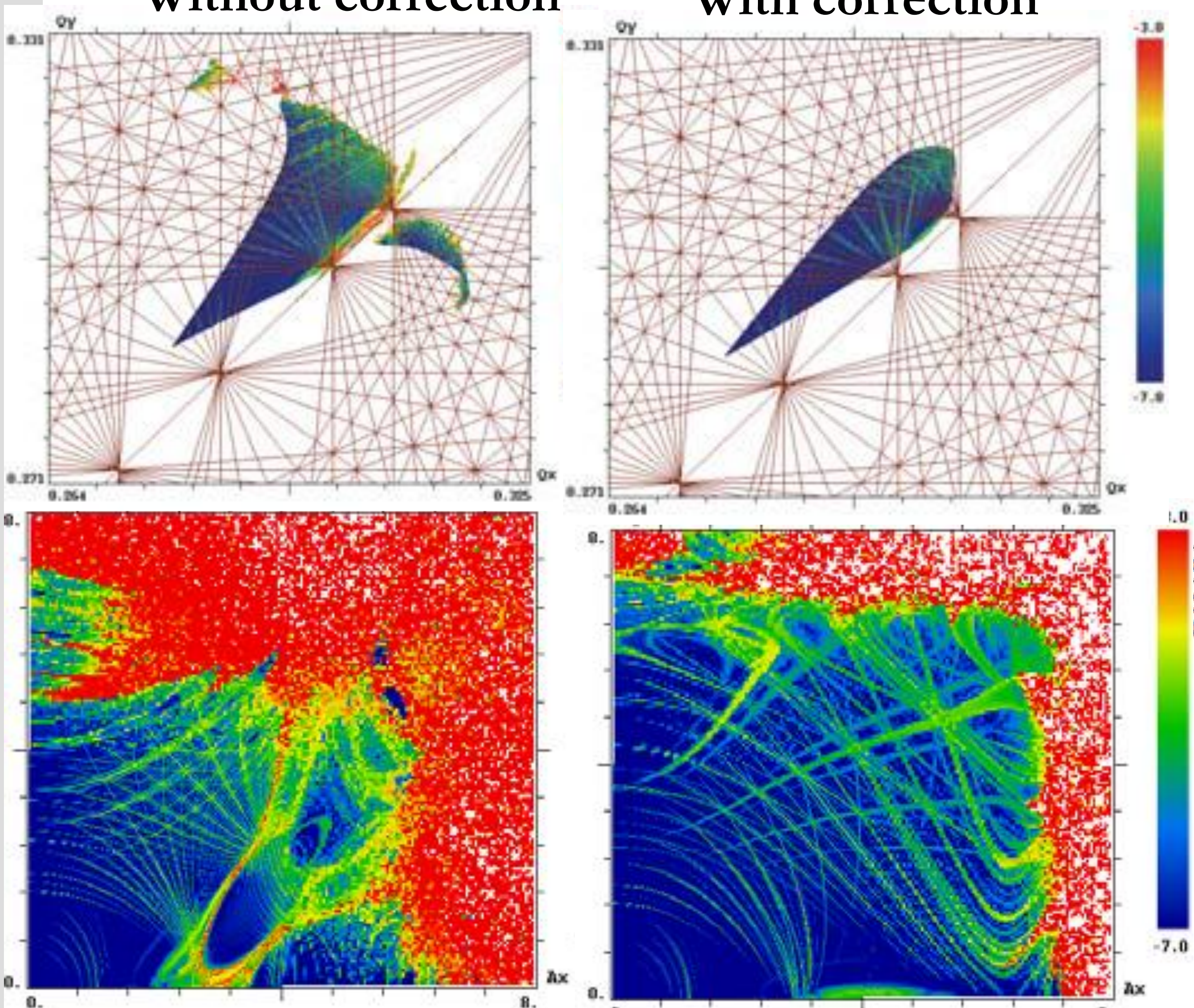

Reduced crossing angle of 450μrad @ 15cm

S. Fartoukh et al., PRSTAB, 2015

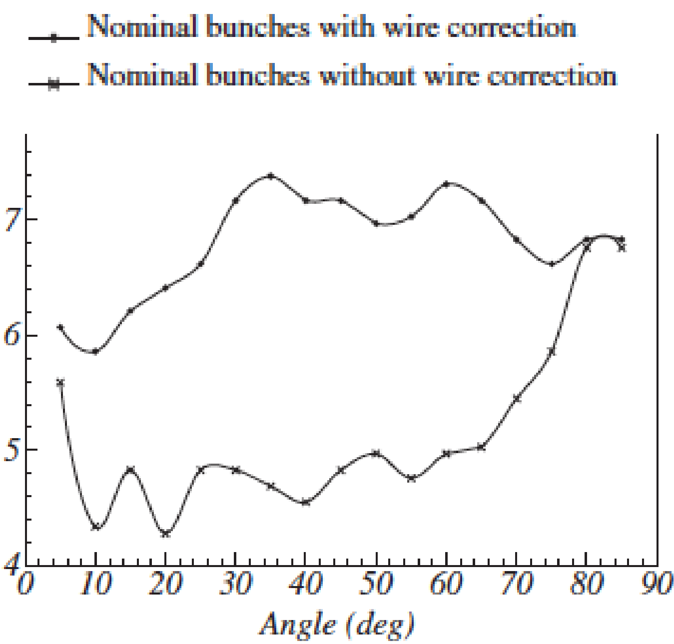

Frequency maps with space-charge

F.Asvesta, H.Bartosik and YP, 2017

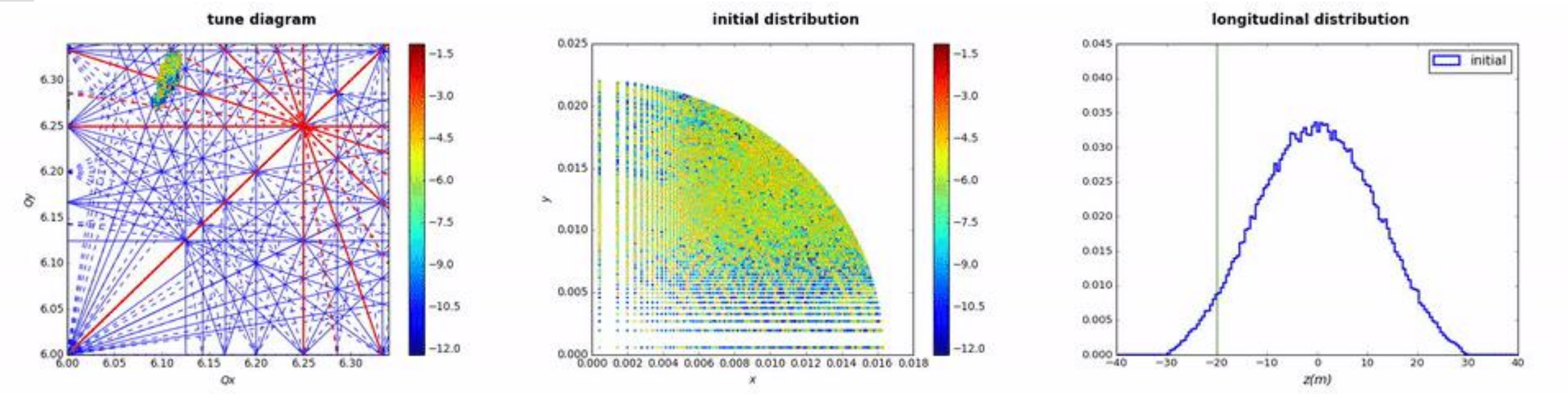

- Evolution of frequency map over different longitudinal position
- Tunes acquired over each longitudinal period
- Particles with similar longitudinal offset but different amplitudes experience the resonance in different manner
- Particles with different longitudinal offset may experience different resonances

Contents of the 2nd lecture

- Resonances and the path to chaos
  - Topology of 3rd and 4th order resonance
  - Path to chaos and resonance overlap
  - Dynamic aperture simulations
- Frequency map analysis
  - NAFF algorithm
  - Aspects of frequency maps
  - Frequency and diffusion maps for the LHC
  - Frequency map for lepton rings
  - Working point choice
  - Beam-beam effect
- Experiments
  - Experimental frequency maps
  - Beam loss frequency maps
  - Space-charge frequency scan

Experimental frequency maps

D. Robin, C. Steier, J. Laskar, and L. Nadolski, PRL 2000

- Frequency analysis of turn-by-turn data of beam oscillations produced by a fast kicker magnet and recorded on a Beam Position Monitors
- Reproduction of the non-linear model of the Advanced Light Source storage ring and working point optimization for increasing beam lifetime

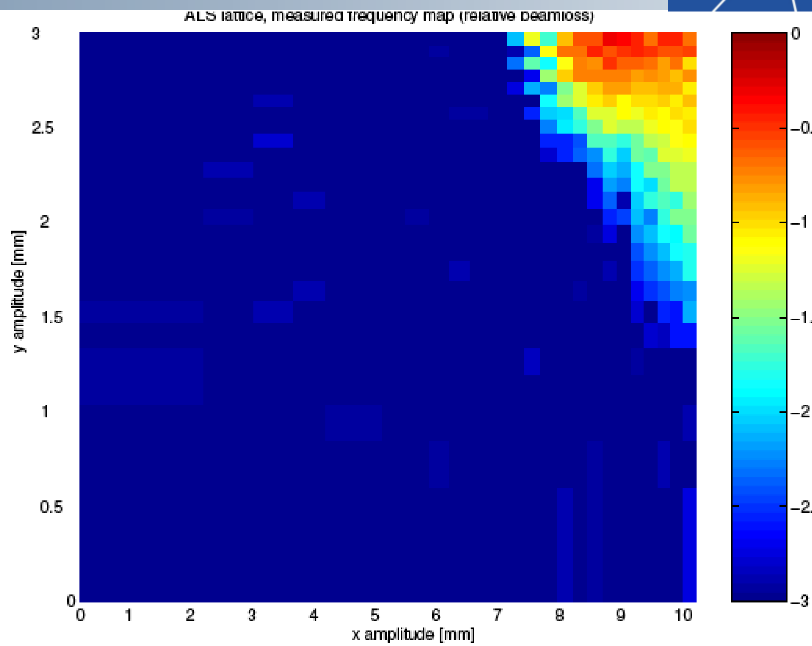

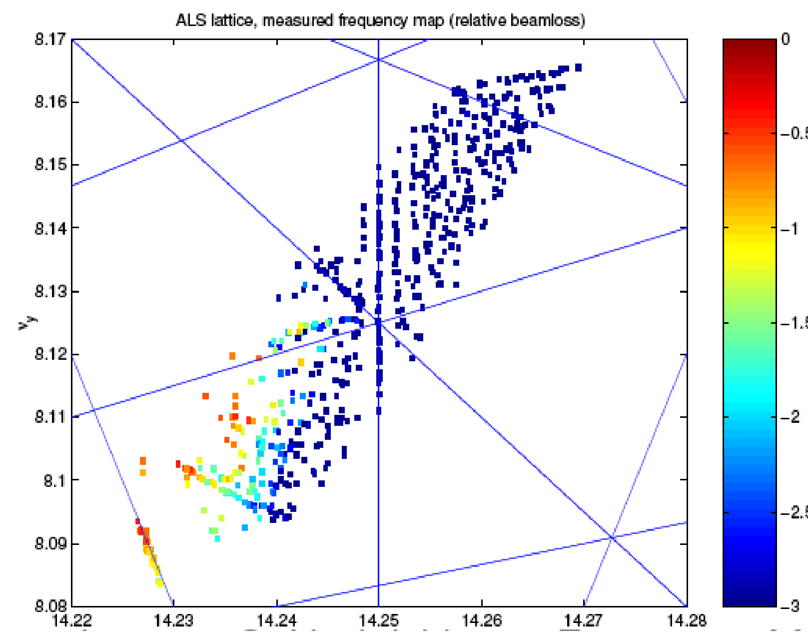

Experimental Methods – Tune scans

- Study the resonance behavior around different working points in SPS
- Strength of individual resonance lines can be identified from the beam loss rate, i.e. the derivative of the beam intensity at the moment of crossing the resonance
- Vertical tune is scanned from about 0.45 down to 0.05 during a period of 3s along the flat bottom
- Low intensity 4-5e10 p/b single bunches with small emittance injected
- Horizontal tune is constant during the same period
- Tunes are continuously monitored using tune monitor (tune post-processed with NAFF) and the beam intensity is recorded with a beam current transformer

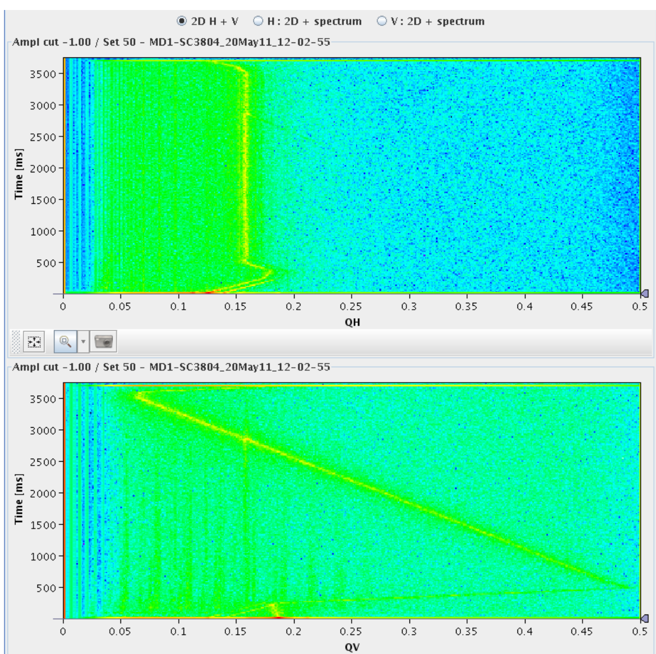

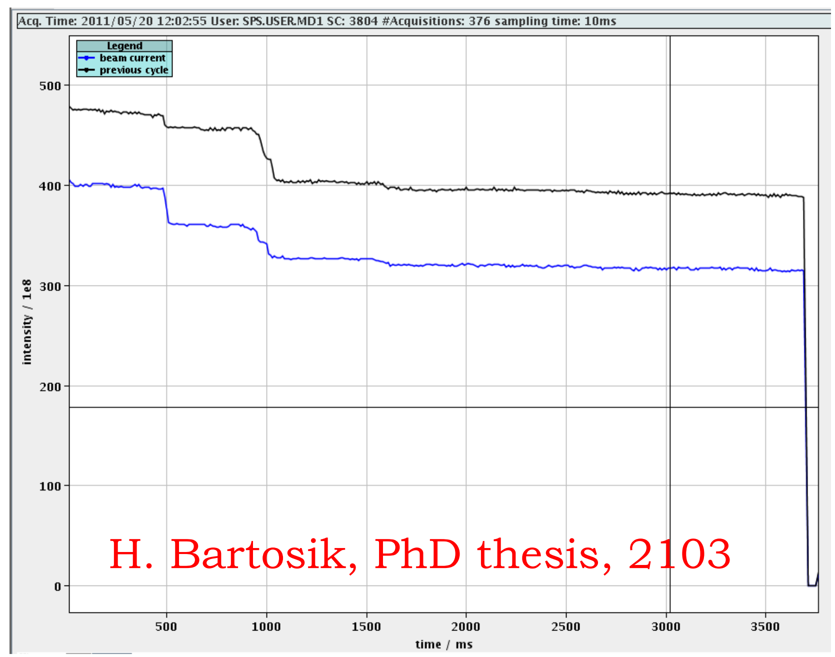

H. Bartosik, PhD thesis, 2103

Tune Scans – Results from the SPS

- Resonances in low γ_t optics
  - Normal sextupole Qx+2Qy is the strongest
  - Skew sextupole 2Qx+Qy quite strong
  - Normal sextupole Qx-2Qy, skew sextupole at 3Qy and 2Qx+2Qy fourth order visible
- Resonances in the nominal optics
  - Normal sextupole resonance Qx+2Qy is the strongest
  - Coupling resonance (diagonal, either Qx-Qy or some higher order of this), Qx-2Qy normal sextupole
  - Skew sextupole resonance 2Qx+Qy weak compared to Q20 case
  - Stop-band width of the vertical integer is stronger (predicted by simulations)

H. Bartosik, PhD thesis, 2103

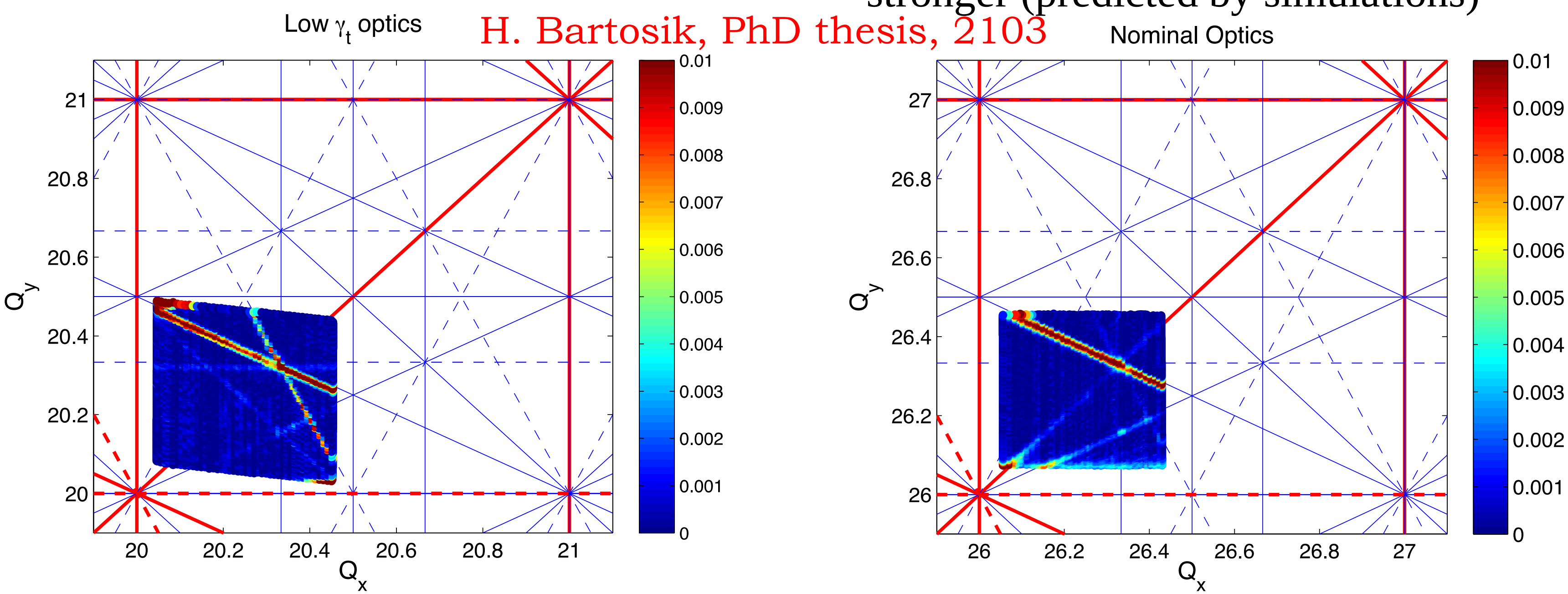

Tune Scans with SC

H.Bartosik

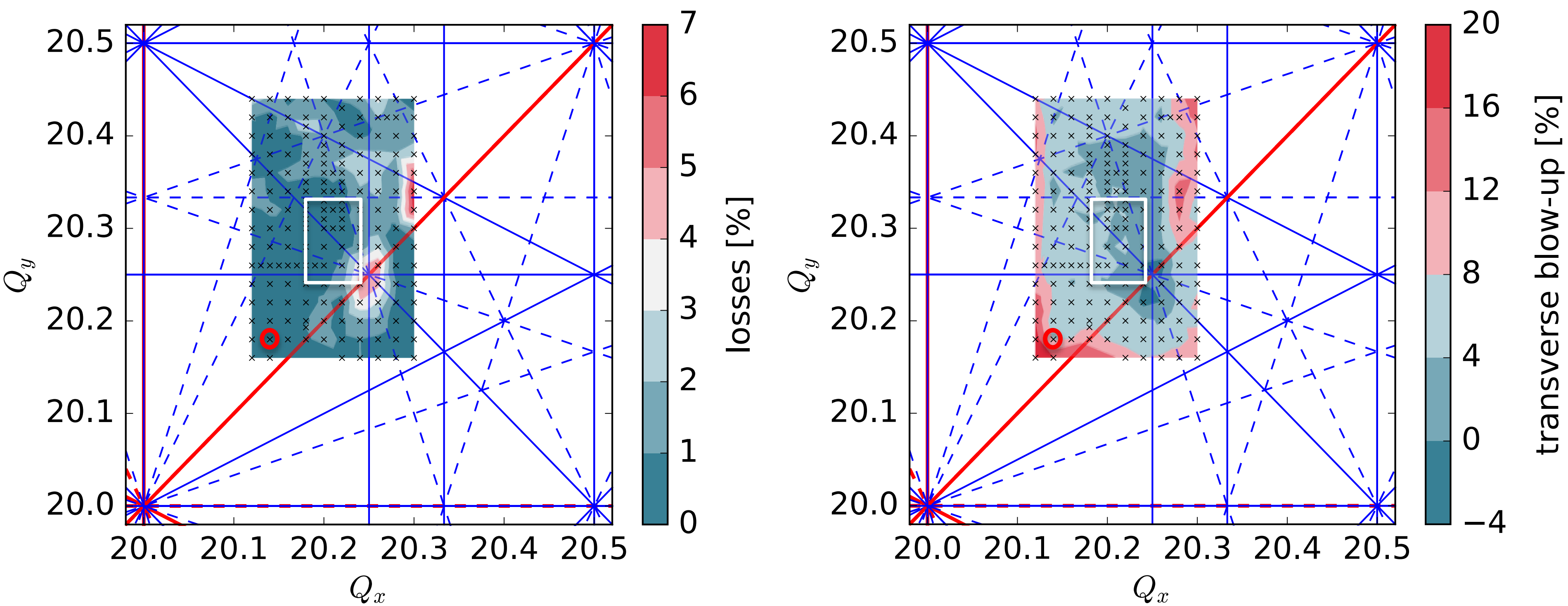

- Limiting resonances for space charge tune spread: (H, V) ~ (0.10, ~0.19)
  - Blow-up at integer resonances as expected
  - Losses for working point close to the Qx + 2Qy normal sextupole resonance (studied in Fix-line experiment with Q26) and around the the 4Qx = 81 normal octupole resonance
- Identified optimum working point area for vertical tune spread of 0.2
  - 20.16 < Qx < 20.23, 20.24 < Qy < 20.33
  - Losses around 0.5% for 3 s storage time on flat bottom

Summary

- Appearance of fixed points (periodic orbits) determine topology of the phase space
- Perturbation of unstable (hyperbolic points) opens the path to chaotic motion
- Resonance can overlap enabling the rapid diffusion of orbits
- Need numerical integration for understanding impact of non-linear effects on particle motion (dynamic aperture)
- Frequency map analysis is a powerful technique for analyzing particle motion in simulations but also in real accelerator experiments

Problems

1) A ring has super-periodicity of 4. Find a relationship for the integer tune that avoids systematic 3rd and 4th order resonances. Generalize this for any super-periodicity.
2) Compute the tune-spread at leading order in perturbation theory for a periodic octupole perturbation in one plane.
3) Extend the previous approach to a general multi-pole.
4) Do skew multi-poles provide 1st order tune-shift with amplitude?

Fixed points for general multi-pole

- For **any polynomial perturbation** of the form x^k the "resonant" Hamiltonian is written as

$$\hat{H}_2 = \delta J_2 + \alpha(J_2) + J_2^{k/2} A_{kp} \cos(k\psi_2)$$

- Note now that **in contrast** to the sextupole there is a non-linear detuning term $\alpha(J_2)$

Fixed points for general multi-pole

- For **any polynomial perturbation** of the form x^k the "resonant" Hamiltonian is written as

$$\hat{H}_2 = \delta J_2 + \alpha(J_2) + J_2^{k/2} A_{kp} \cos(k\psi_2)$$

- Note now that **in contrast** to the sextupole there is a non-linear detuning term $\alpha(J_2)$
- The conditions for the fixed points are

$$\sin(k\psi_2) = 0 \ , \quad \delta + \frac{\partial \alpha(J_2)}{\partial J_2} + \frac{k}{2} J_2^{k/2-1} A_{kp} \cos(k\psi_2) = 0$$

- There are k **fixed points** for which $\cos(k\psi_{20}) = -1$ and the fixed points are **stable** (elliptic). They are surrounded by ellipses
- There are also k **fixed points** for which $\cos(k\psi_{20}) = 1$ and the fixed points are **unstable** (hyperbolic). The trajectories are hyperbolas

Fixed points for an octupole

- The resonant Hamiltonian close to the **4th order resonance** is written as

$$\hat{H}_2 = \delta J_2 + c J_2^2 + J_2^2 A_{kp} \cos(4\psi_2)$$

- The **fixed points** are found by taking the derivative over the two variables and setting them to zero, i.e.

$$\sin(4\psi_2) = 0 \ , \quad \delta + 2cJ_2 + 2J_2 A_{kp} \cos(4\psi_2) = 0$$

- The fixed points are at

$$\psi_{20} = \frac{\pi}{4}, \frac{\pi}{2}, \frac{3\pi}{4}, \pi, \frac{5\pi}{4}, \frac{3\pi}{2}, \frac{7\pi}{4}, 2\pi$$

- For **half** of them, there is a minimum in the potential as $\cos(4\psi_{20}) = -1$ and they are **elliptic** and **half** of them they are **hyperbolic** as $\cos(4\psi_{20}) = 1$